Journal of Circuits, Systems, and Computers
Vol. 18, No. 4 (2009) 733–769


World Scientific
www.worldscientific.com

# MOS-C KHN FILTER USING VOLTAGE OP AMP, CFOA, OTRA AND DCVC

AHMED M. SOLIMAN

*Electronics and Communication Engineering Department, Faculty of Engineering, Cairo University, Egypt*
*asoliman@ieee.org*

AHMED H. MADIAN

*Engineering Department, National Center for Radiation and Research Technology, Egyptian Atomic Energy Authority, Cairo, Egypt*
*ah_madian@hotmail.com*

Revised 9 February 2009

MOS-C realizations of the Kerwin–Huelsman–Newcomb (KHN) circuit using the commercially available Voltage Operational Amplifier (VOA) and the Current Feedback Operational Amplifier (CFOA) are reviewed in this paper. Additional MOS-C KHN realizations using the Operational Transresistance Amplifier (OTRA) and the Differential Current Voltage Conveyor (DCVC) are also included. MOS-C realizations of the KHN circuit using CMOS operational amplifier, CMOS current feedback operational amplifier and CMOS operational transresistance amplifier are also given.

Spice simulation results using 0.18 CMOS technology model from MOSIS are included together with detailed comparison tables to demonstrate the differences between MOS-C KHN circuits using both of the commercially available active building blocks and CMOS integrated building blocks. A comparison with the Gm-C KHN circuit is also included.

*Keywords*: Kerwin–Huelsman–Newcomb filter; CFOA; OTRA; DCVC.

## 1. Introduction

The Kerwin–Huelsman–Newcomb (KHN)[1] second-order filter using operational amplifiers is one of the most popular universal circuits and has appeared in many text books.[2–5] Recently the progress in the KHN circuit realization has been reviewed in Ref. 6. It is well known that the classical KHN circuit using Op Amps has frequency limitations due to the finite gain-bandwidth of the Op Amps.[2] Passive and active compensation methods to improve the circuit performance for high $Q$ designs were also reviewed in Ref. 6.

In this paper, the progress in the realization of the MOS-C KHN circuit using the commercially available voltage operational amplifier (VOA), the current feedback

operational amplifier (CFOA), operational transresistance amplifiers (OTRA), the differential current voltage conveyor (DCVC) is reviewed. The OTRA and the DCVC are realized using two CFOA. MOS-C realizations of the KHN circuit using CMOS operational amplifier, CMOS current feedback operational amplifier and CMOS operational transresistance amplifier are also given. Spice simulation results using 0.18 CMOS technology model from MOSIS are included and detailed comparison tables summarizing the differences between MOS-C KHN circuits are included.

## 2. The KHN Circuit Using Op Amps

Figure 1 represents the classical KHN circuit using three Op Amps.[1] The transfer functions at the circuit three outputs are given by:

$$\frac{V_{\mathrm{HP}}}{V_{in}} = \frac{\frac{2R_4}{R_3+R_4}s^2}{s^2 + \frac{2R_3}{R_3+R_4}\cdot\frac{s}{R_1C_1} + \frac{1}{R_1R_2C_1C_2}}, \tag{1}$$

$$\frac{V_{\mathrm{BP}}}{V_{in}} = \frac{-\frac{2R_4}{R_3+R_4}\frac{s}{R_1C_1}}{s^2 + \frac{2R_3}{R_3+R_4}\cdot\frac{s}{R_1C_1} + \frac{1}{R_1R_2C_1C_2}}, \tag{2}$$

$$\frac{V_{\mathrm{LP}}}{V_{in}} = \frac{\frac{2R_4}{R_3+R_4}\frac{1}{R_1R_2C_1C_2}}{s^2 + \frac{2R_3}{R_3+R_4}\cdot\frac{s}{R_1C_1} + \frac{1}{R_1R_2C_1C_2}}. \tag{3}$$

The above equations are based on equal values for $R_5$ and $R_6$. The circuit is usually designed by taking equal capacitors $C_1 = C_2 = C$ and the design equations are given by:

$$R_1 = R_2 = \frac{1}{\omega_0 C}, \quad R_4 = (2Q-1)R_3. \tag{4}$$

It is seen that there is independent control on $Q$ by adjusting the value of $R_4$ without affecting $\omega_0$ of the filter. The magnitude of the gain at $\omega_0$ at any of the

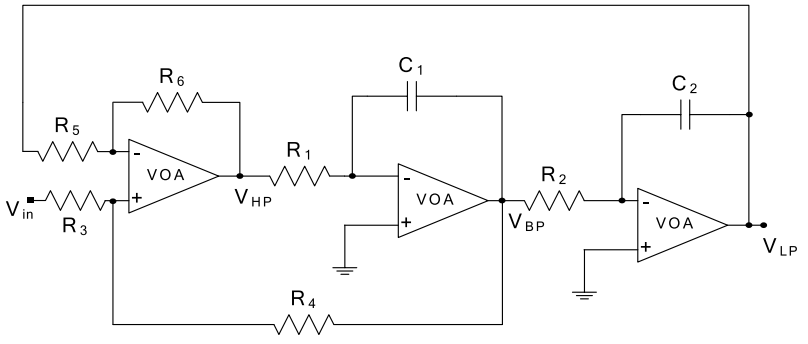


Fig. 1. The Kerwin–Huelsman–Newcomb filter.[1]

three outputs of the filter is given by $(2Q-1)$ and there is no independent control on the gain.

## 3. The MOS Transistor Nonlinearities Cancellation Methods

An NMOS transistor is shown in Fig. 2(a), with its gate connected to a control voltage $V_G$. The terminal voltages $V_1$ and $V_2$ are assumed to remain below $V_G$ by at least the threshold voltage of the transistor $V_T$ to allow operation in the non-saturation region. The current in the non-saturation region is given by Refs. 7 and 8:

$$I = K(V_G - V_T)(V_1 - V_2) + a_1(V_1^2 - V_2^2) + a_2(V_1^3 - V_2^3) + \cdots , \tag{5}$$

$K$ is the transconductance parameter of the NMOS transistor and is given by

$$K = \mu_n C_{OX} \left( \frac{W}{L} \right), \tag{6}$$

where $(W/L)$ is the transistor aspect ratio, $C_{OX}$ is the gate oxide capacitance per unit area and $\mu_n$ is the electron mobility.

Many different techniques have been proposed for eliminating the effect of the nonlinearities.[7,8] The two methods of nonlinearity cancellation that are used in this paper are shown in Figs. 2(b) and 2(c).

The circuit shown in Fig. 2(b) accomplishes in principle complete cancellation of both the even and odd nonlinearities in the difference between the currents of

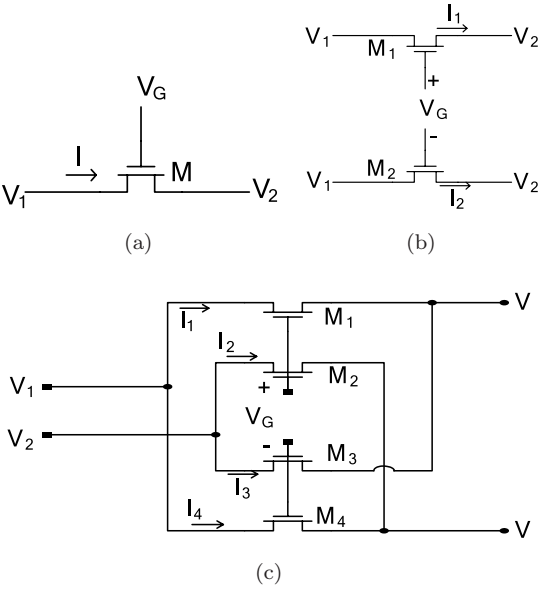


Fig. 2. (a) The symbol of NMOS transistor, (b) Two MOS transistors circuit with full nonlinearities' cancellation, (c) Four MOS transistors circuit with full nonlinearities' cancellation.[7,8]

$M_1$ and $M_2$. Since the transistors $M_1$ and $M_2$ have equal drain and source voltages, therefore the difference between two currents is given by

$$I = I_1 - I_2 = KV_G(V_1 - V_2) \quad \text{for } V_G - V_T \geq \max(V_1, V_2)\,. \tag{7}$$

The circuit shown in Fig. 2(c)[7,8] also performs a complete cancellation of the nonlinearities and the linear current is given by

$$I = (I_1 + I_3) - (I_2 + I_4) = KV_G(V_1 - V_2) \quad \text{for } V_G - V_T \geq \max(V, V_1, V_2)\,. \tag{8}$$

In the following sections the MOS-C KHN circuits using the VOA, CFOA, OTRA and DCVC are considered together with detailed simulation and comparison tables. The OTRA and the DCVC are realized using the commercially available CFOA AD844-available from Ref. 9.

## 4. MOS-C KHN Circuit Using VOA

The first MOS-C KHN circuit using VOA was introduced in Ref. 10 and is based on the modified KHN circuit shown in Fig. 3(a). The circuit equations are given by:

$$\frac{V_{\mathrm{HP}}}{V_{in}} = \frac{s^2 \frac{G_3}{G_6}}{s^2 + s\frac{G_1 G_4}{C_1 G_6} + \frac{G_1 G_2 G_5}{C_1 C_2 G_6}}\,, \tag{9}$$

$$\frac{V_{\mathrm{BP}}}{V_{in}} = \frac{-s\frac{G_1 G_3}{C_1 G_6}}{s^2 + s\frac{G_1 G_4}{C_1 G_6} + \frac{G_1 G_2 G_5}{C_1 C_2 G_6}}\,, \tag{10}$$

$$\frac{V_{\mathrm{LP}}}{V_{in}} = \frac{\frac{G_1 G_2 G_3}{C_1 C_2 G_6}}{s^2 + s\frac{G_1 G_4}{C_1 G_6} + \frac{G_1 G_2 G_5}{C_1 C_2 G_6}}\,. \tag{11}$$

Using the four MOS transistor cell in Fig. 2(c) to replace each pair of equal resistors and taking:

$$G_i = K_i V_{G_i}\,, \quad \text{where } (i = 1 \text{ to } 6). \tag{12}$$

The transfer functions are given by:

$$\frac{V_{\mathrm{HP}}}{V_{in}} = \frac{s^2 \frac{K_3 V_{G3}}{K_6 V_{G6}}}{s^2 + s\frac{K_1 K_4 V_{G1} V_{G4}}{C_1 K_6 V_{G6}} + \frac{K_1 K_2 K_5 V_{G1} V_{G2} V_{G5}}{C_1 C_2 K_6 V_{G6}}}\,, \tag{13}$$

$$\frac{V_{\mathrm{BP}}}{V_{in}} = \frac{-s\frac{K_1 K_3 V_{G1} V_{G3}}{C_1 K_6 V_{G6}}}{s^2 + s\frac{K_1 K_4 V_{G1} V_{G4}}{C_1 K_6 V_{G6}} + \frac{K_1 K_2 K_5 V_{G1} V_{G2} V_{G5}}{C_1 C_2 K_6 V_{G6}}}\,, \tag{14}$$

$$\frac{V_{\mathrm{LP}}}{V_{in}} = \frac{\frac{K_1K_2K_3V_{G1}V_{G2}V_{G3}}{C_1C_2K_6V_{G6}}}{s^2 + s\frac{K_1K_4V_{G1}V_{G4}}{C_1K_6V_{G6}} + \frac{K_1K_2K_5V_{G1}V_{G2}V_{G5}}{C_1C_2K_6V_{G6}}}\,. \tag{15}$$

Taking $V_{G5} = V_{G6}$ and for equal $K$ values, the $\omega_0$, $Q$ and gain are given by:

$$\omega_0 = K\sqrt{\frac{V_{G1}\cdot V_{G2}}{C_1C_2}}\,, \quad Q = \frac{V_{G6}}{V_{G4}}\sqrt{\frac{C_1V_{G2}}{C_2V_{G1}}}\,. \tag{16}$$

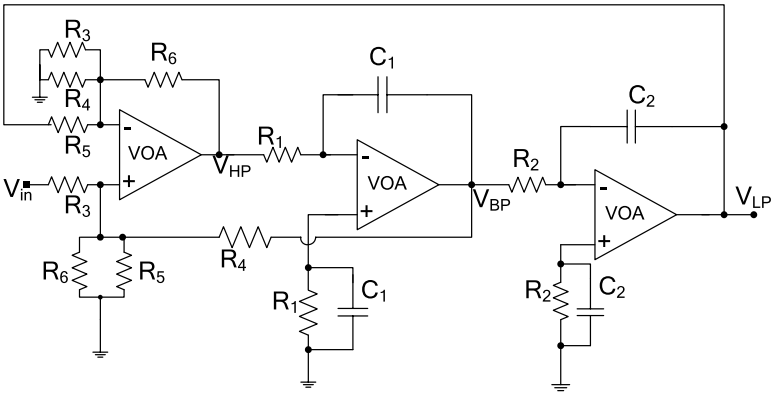


Fig. 3(a). Modified active RC KHN circuit.[10]

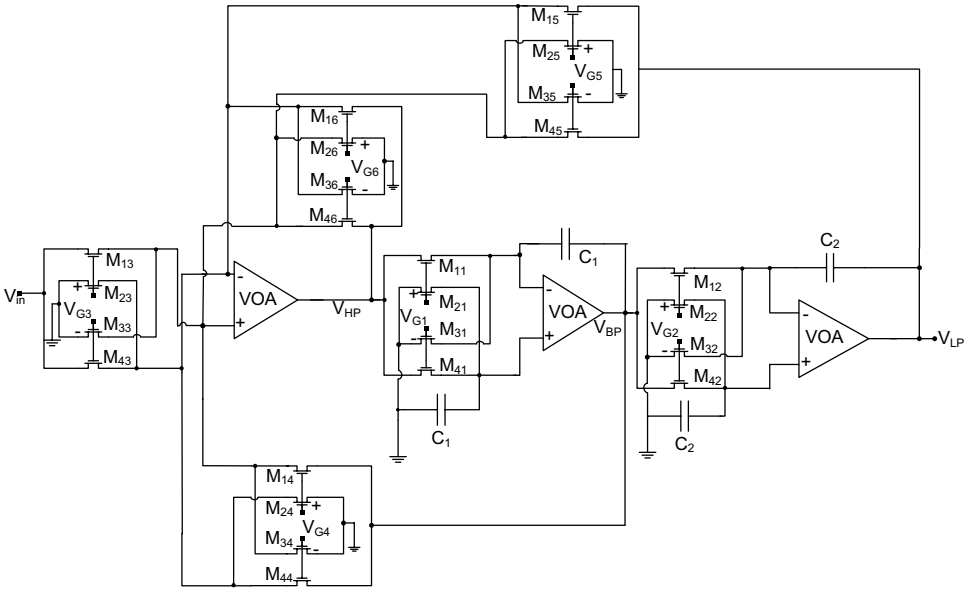


Fig. 3(b). MOSFET-C KHN filter structure using LM741 as VOA.

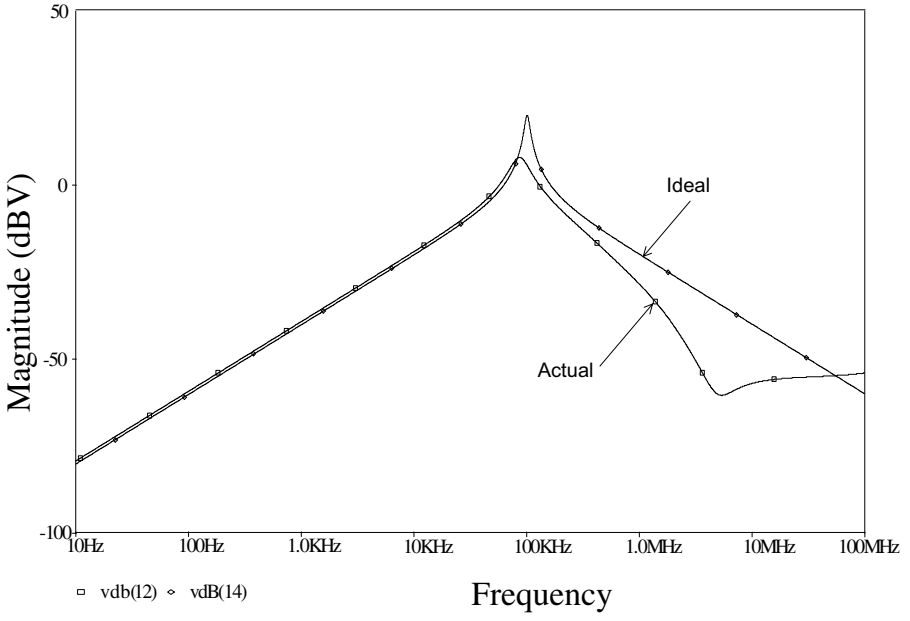


Fig. 3(c). Ideal and actual magnitude responses of KHN using LM741 as VOA and MOS-C with $Q = 10$, $f_0 = 100\,\text{KHz}$.

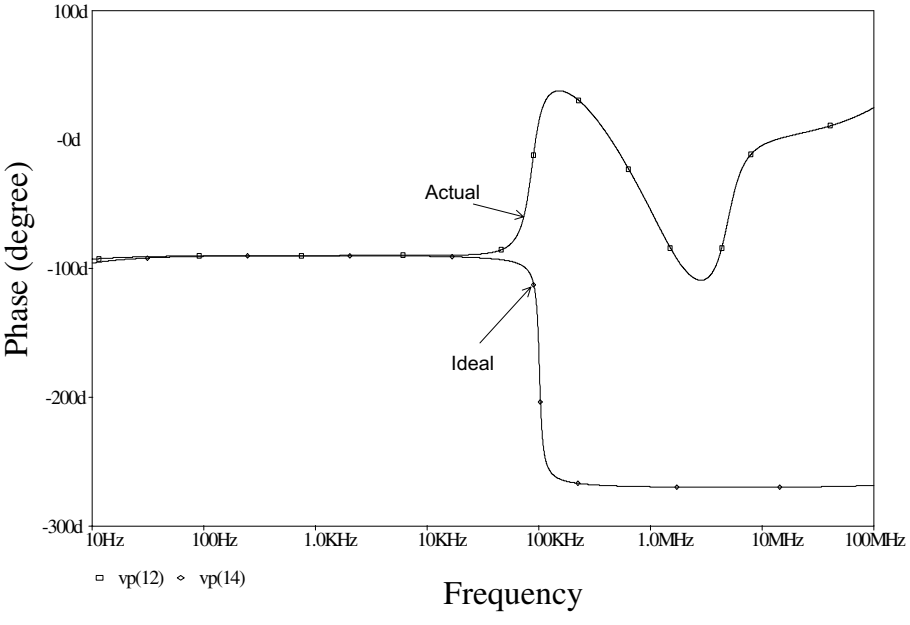


Fig. 3(d). Ideal and actual phase response of the band-pass KHN using LM741 as VOA and MOS-C with $f_0 = 100\,\text{KHz}$.

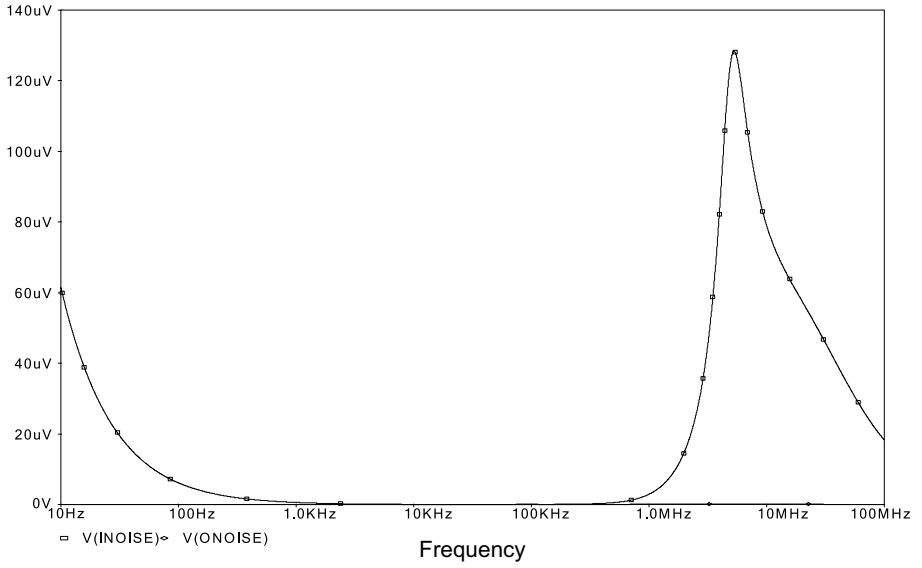


Fig. 3(e). The input/output referred noise of the KHN circuit of Fig. 3(b).

The gain at $\omega_0$ at each of the three outputs is given by:

$$\text{Gain at } \omega_0 = \frac{V_{G3}}{V_{G4}}. \tag{17}$$

It is seen that $V_{G3}$ controls the gain without affecting $\omega_0$ or $Q$.

The PSpice simulations have been carried out using 0.18 CMOS technology model from MOSIS to realize a band-pass response with $f_0 = 100\,\text{kHz}$, center frequency gain of 10 and $Q = 10$. The design values of the circuit parameters are $C_1 = C_2 = 545\,\text{pF}$. The transistor aspect ratios $(W/L) = (2\,\mu\text{m}/4\,\mu\text{m})$, $K^{\backslash} = 251.497\,\mu\text{A/V}^2$, and the gate voltages have been taken as $V_{G1} = V_{G2} = V_{G3} = V_{G5} = V_{G6} = 2.748\,\text{V}$ and $V_{G4} = 0.2748\,\text{V}$. For the VOA the exact model of LM 741 is used with supply voltages of $\pm 12\,\text{V}$.

Figures 3(c) and 3(d) shows the magnitude and phase responses of the simulated and the ideal responses respectively. From the simulations it is seen that the VOA frequency limitations results in large deviation from the ideal response. Figure 3(e) shows the input/output referred noise.

### 4.1. *MOS-C inverted KHN circuit using VOA*

Figure 4(a) represents the inverting input KHN circuit[11] which realizes the three outputs with opposite polarities to the classical KHN of Fig. 1. The circuit uses one resistor more than the circuit of Fig. 1. For $R_3 = R_5 = R_6$ and taking equal capacitors $C_1 = C_2 = C$ and the design equations are given by Ref. 6:

$$R_1 = R_2 = \frac{1}{\omega_0 C}\,, \quad R_4 = (3Q-1)R_7\,. \tag{18}$$

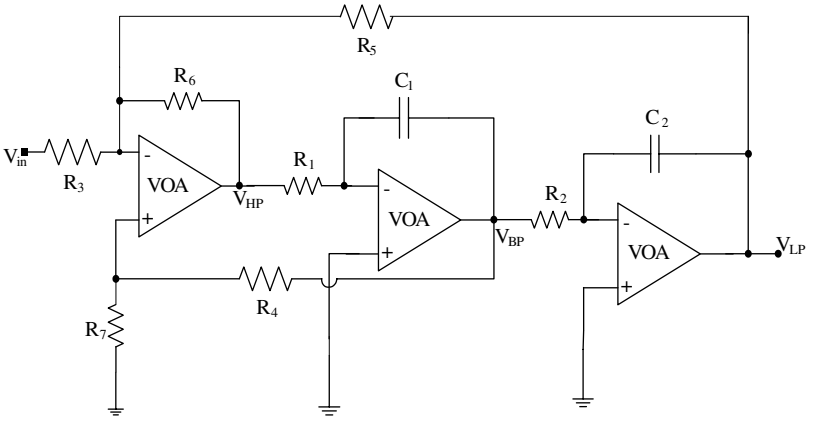


Fig. 4(a). Active RC inverting KHN.[11]

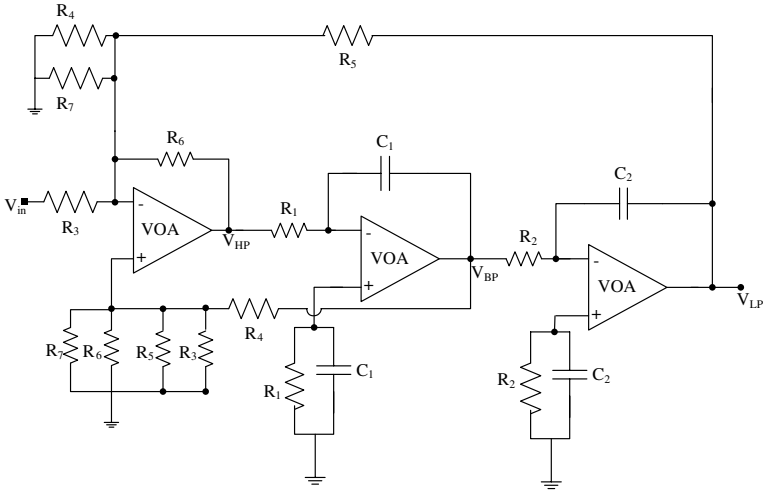


Fig. 4(b). Modified active RC inverting KHN.

It is seen that there is independent control on $Q$ by adjusting the value of $R_4$ without affecting $\omega_0$ of the filter. The magnitude of the gain at $\omega_0$ at any of the three outputs of the filter is given by $(3Q-1)$ and there is no independent control on the gain.

In order to generate the MOS-C circuit an intermediate step is needed resulting in the modified circuit shown in Fig. 4(b). It is seen that the two grounded resistors $R_7$ connected to the two Op Amp input terminals can be safely removed from the circuit of Fig. 4(b). Using the four MOS transistor cell of Fig. 2(c) to replace each of the two equal resistors results in the MOS-C inverting KHM circuit shown in Fig. 4(c).

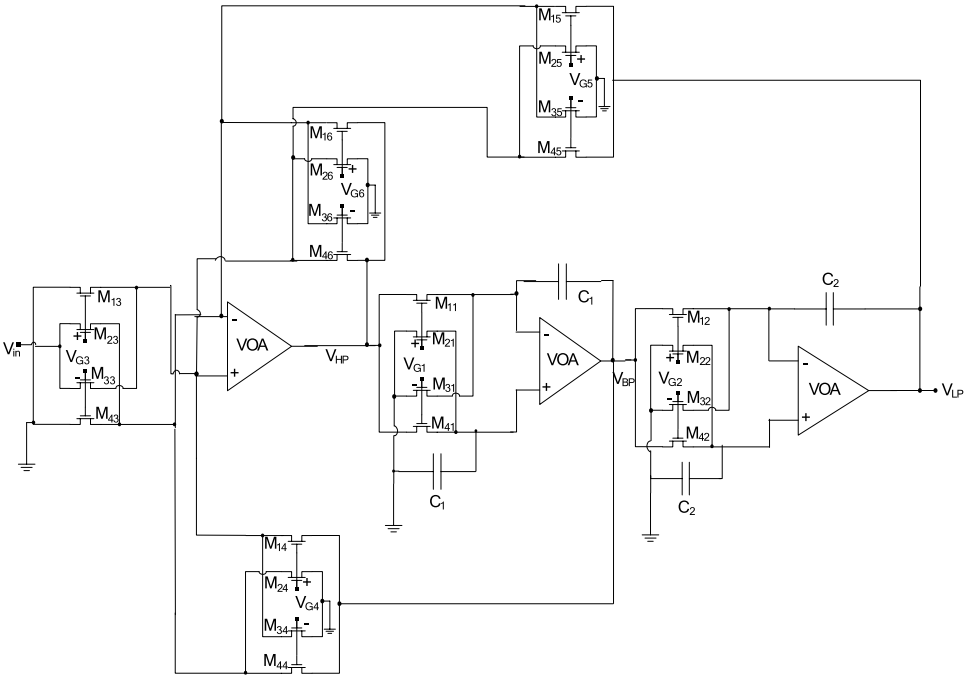


Fig. 4(c). MOSFET-C inverting KHN filter structure using LM741 as VOA.

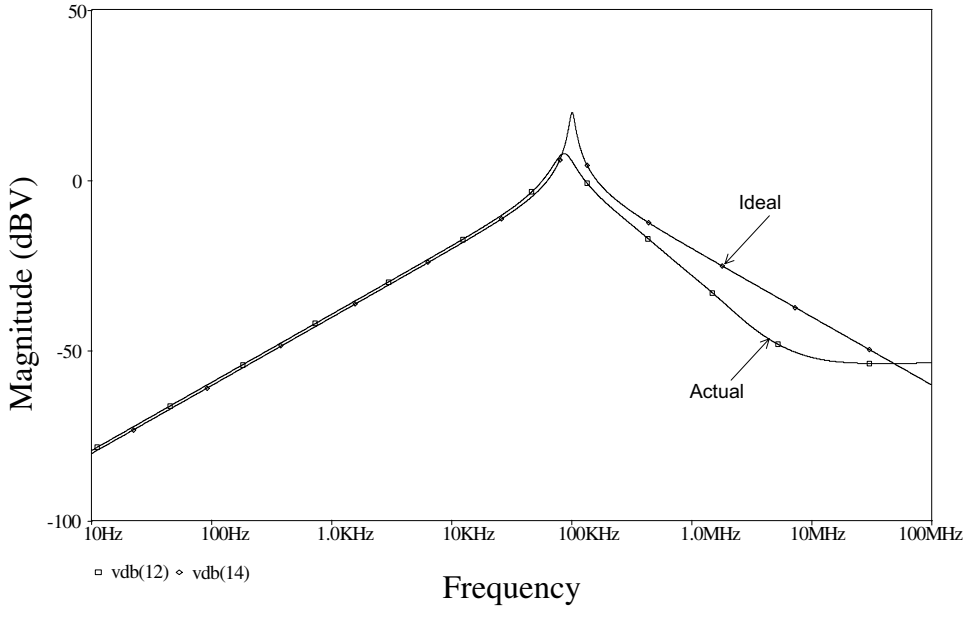


Fig. 4(d). Ideal and actual magnitude responses of inverting KHN using LM741 as VOA and MOS-C with $Q = 10$, $f_0 = 100\,\text{KHz}$.

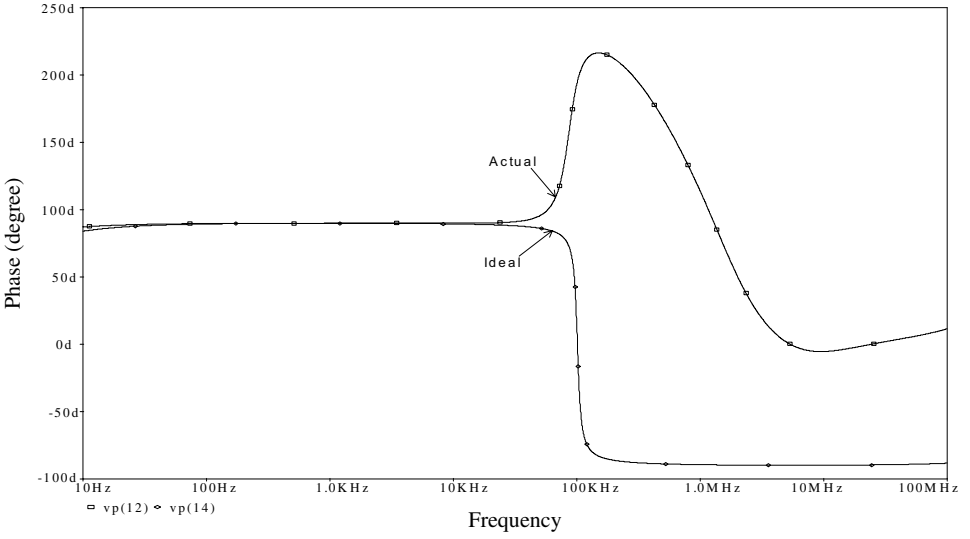


Fig. 4(e). Ideal and actual phase response of the band-pass inverting KHN using LM741 as VOA and MOS-C with $f_0 = 100\,\text{KHz}$.

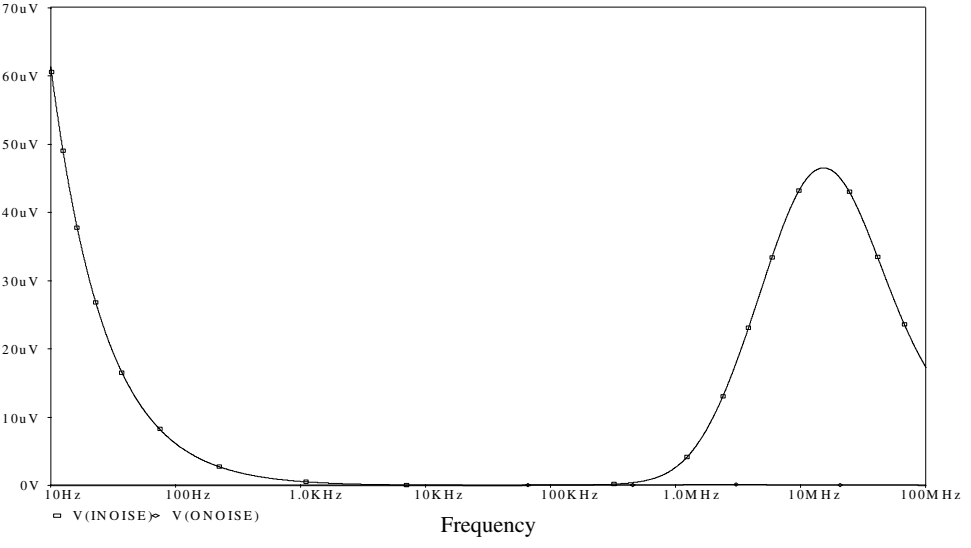


Fig. 4(f). The input/output referred noise of the inverting KHN circuit of Fig. 4(c).

For $V_{G5} = V_{G6}$ and for equal $K$, the circuit equations are given by:

$$\frac{V_{\text{HP}}}{V_{in}} = \frac{-s^2 \frac{V_{G3}}{V_{G6}}}{s^2 + s\frac{KV_{G1}V_{G4}}{C_1 V_{G6}} + \frac{K^2 V_{G1}V_{G2}}{C_1 C_2}}, \tag{19}$$

Table 1. The eight possible sign combination of the polarities of the KHN circuit.

| $V_{Gi}$ polarity | | | | | | Output polarity | | |
|---|---|---|---|---|---|---|---|---|
| $V_{G1}$ | $V_{G2}$ | $V_{G3}$ | $V_{G4}$ | $V_{G5}$ | $V_{G6}$ | HP | BP | LP |
| + | + | + | + | + | + | + | − | + |
| + | + | + | − | − | − | − | + | − |
| − | − | + | + | − | − | − | − | − |
| − | − | + | − | + | + | + | + | + |
| + | − | + | − | + | − | − | + | + |
| + | − | + | + | − | + | + | − | − |
| − | + | + | − | − | + | + | + | − |
| − | + | + | + | + | − | − | − | + |

$$\frac{V_{\mathrm{BP}}}{V_{in}} = \frac{s\frac{KV_{G1}V_{G3}}{C_1V_{G6}}}{s^2 + s\frac{KV_{G1}V_{G4}}{C_1V_{G6}} + \frac{K^2V_{G1}V_{G2}}{C_1C_2}}, \tag{20}$$

$$\frac{V_{\mathrm{LP}}}{V_{in}} = \frac{-\frac{K^2V_{G1}V_{G2}V_{G3}}{C_1C_2V_{G6}}}{s^2 + s\frac{KV_{G1}V_{G4}}{C_1V_{G6}} + \frac{K^2V_{G1}V_{G2}}{C_1C_2}}. \tag{21}$$

It is interesting to notice that this circuit is similar to the MOS-C KHN circuit of Fig. 3(b) with the interchange of $V_{in}$ and ground at the NMOS cell number 3.

It is worth noting that four alternative sign combinations of the high-pass, band-pass and low-pass polarities can be obtained by proper choice of the signs of $V_{Gi}$ ($i = 1$ to 6). Each sign combination is obtained two times one with $V_{G3}$ positive and the other with $V_{G3}$ negative.

The complete set of the eight sign combinations can only be obtained with unequal $V_{G5}$ and $V_{G6}$ as demonstrated in Table 1.

## 5. MOS-C KHN Circuit Using CFOA

The current-feedback operational amplifier (CFOA) is a four-port network[12,13] with a describing matrix of the form

$$\begin{bmatrix} I_Y \\ V_X \\ I_Z \\ V_O \end{bmatrix} = \begin{bmatrix} 0 & 0 & 0 & 0 \\ 1 & 0 & 0 & 0 \\ 0 & 1 & 0 & 0 \\ 0 & 0 & 1 & 0 \end{bmatrix} \begin{bmatrix} V_Y \\ I_X \\ V_Z \\ I_O \end{bmatrix}. \tag{22}$$

The application of the CFOA in the realization of MOS-C KHN circuit is considered in the following two sections.

### 5.1. *MOS-C KHN circuit using CFOA as a three-terminal device*

In this section the CFOA is used as a three-port network leaving the $Z$ port open circuit.

In this case the CMOS-C KHN circuit shown in Fig. 5(a) is similar to the VOA circuit and the circuit equations are the same as given by Eqs. (13)–(17).

The PSpice simulations have been carried out for the circuit of Fig. 5(a) using the same design values as in the previous section. For the CFOA the exact model of AD844 is used with supply voltages of ±5 V.

Figures 5(b) and 5(c) show the magnitude and phase responses of the simulated and the ideal responses respectively. From the simulations of the KHN using the CFOA as a three terminal device, it is seen that the requirements of the required filter are nearly satisfied. Figure 5(d) shows the input/output referred noise.

### 5.2. *MOS-C KHN circuit using CFOA as four-terminal device*

In this section the CFOA is used as a four-port network utilizing the Z port.

A new CMOS-C KHN circuit is shown in Fig. 6(a) and it uses two grounded capacitors and six MOS resistor circuits and the circuit equations are the same as given by Eqs. (13)–(17). The PSpice simulations have been carried out for the circuit of Fig. 6(a) using the same design values as in the previous section. For the CFOA the exact model of AD844 is used with supply voltages of ± 5 V.

Figures 6(b) and 6(c) show the magnitude and phase responses of the simulated and the ideal responses respectively. From the simulations of the KHN using the

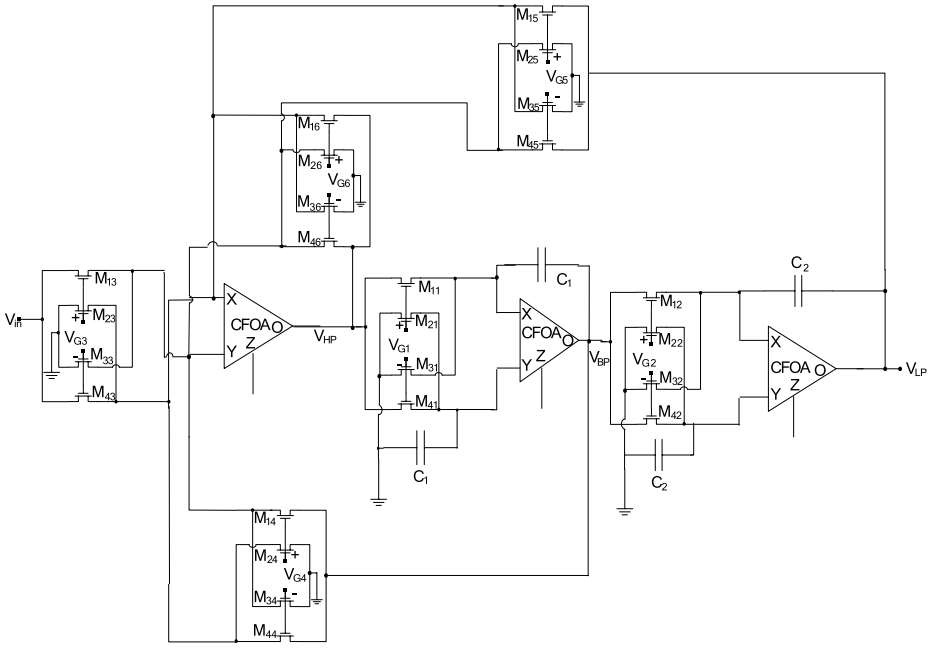


Fig. 5(a). KHN filter using CFOA as three-terminals and MOS-C.

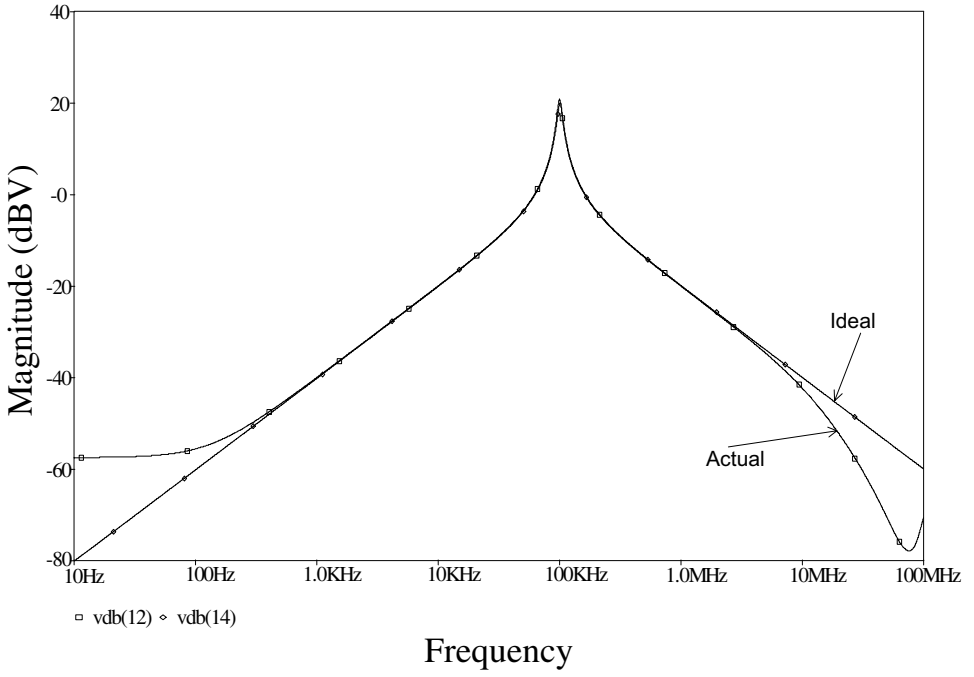


Fig. 5(b). Ideal and actual magnitude responses of KHN using AD844 as VOA and MOS-C with $Q = 10$, $f_0 = 100\,\text{KHz}$.

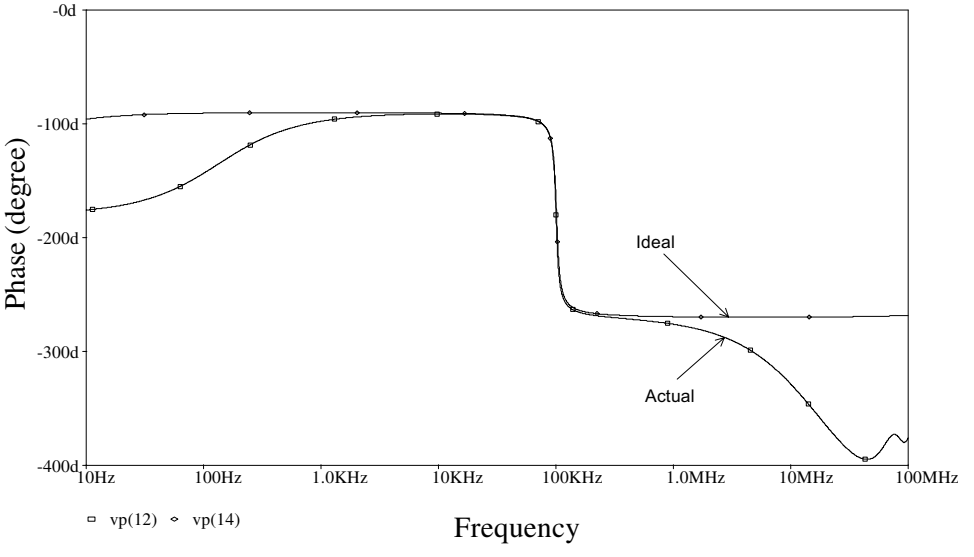


Fig. 5(c). Ideal and actual phase response of the band-pass KHN using AD844 as VOA and MOS-C with $f_0 = 100\,\text{KHz}$.

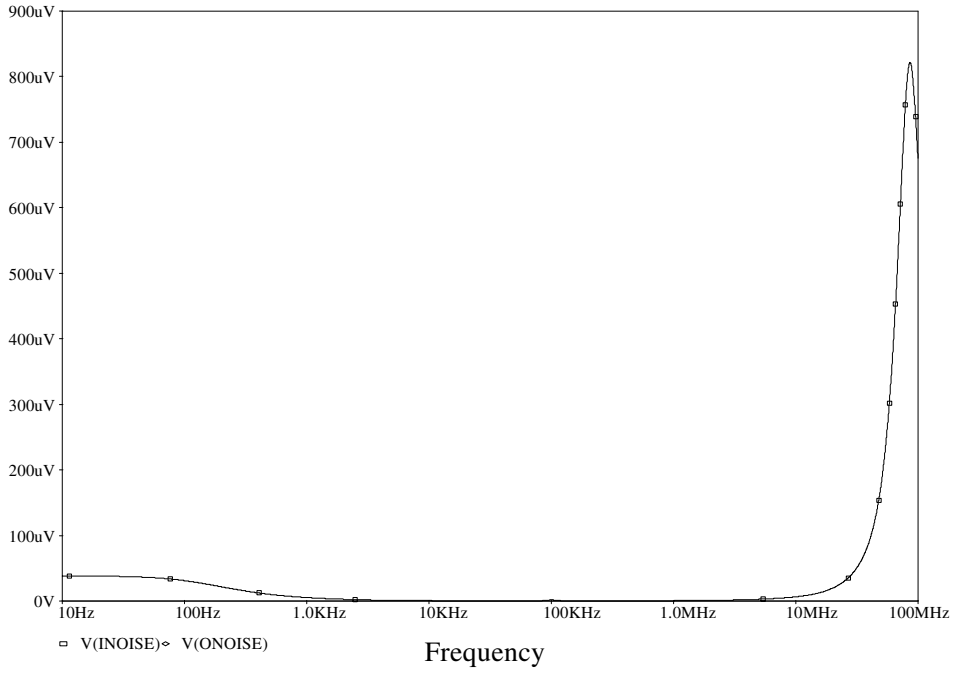


Fig. 5(d). The input/output referred noise of the KHN circuit of Fig. 5(a).

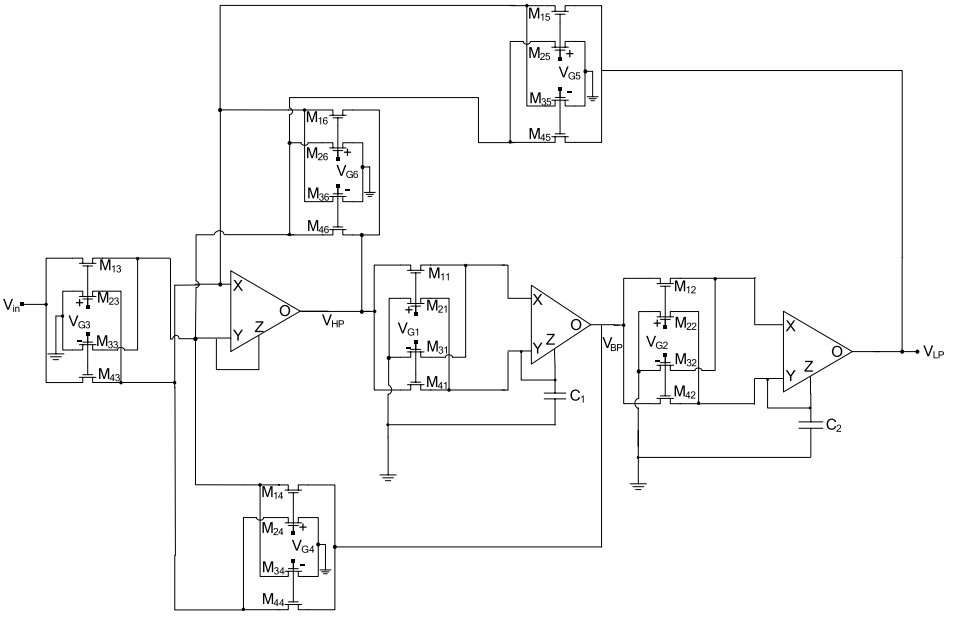


Fig. 6(a). KHN filter using CFOA and MOS-C.

CFOA as a three terminal device it is seen that the requirements of the required filter are nearly satisfied.

Figure 6(d) shows the input/output referred noise.

## 6. MOS-C KHN Circuit Using OTRA

The operational transresistance amplifier (OTRA) shown symbolically in Fig. 7(a) is a three-terminal analog building block that is defined by the following matrix equation:

$$\begin{bmatrix} V_+ \\ V_- \\ V_o \end{bmatrix} = \begin{bmatrix} 0 & 0 & 0 \\ 0 & 0 & 0 \\ R_m & -R_m & 0 \end{bmatrix} \begin{bmatrix} I_+ \\ I_- \\ I_o \end{bmatrix}. \tag{23}$$

$R_m$ is the transresistance gain.

Both the input and output terminals are characterized by low impedance. The input terminals are virtually grounded leading to circuits that are insensitive to stray capacitances. Ideally the transresistance gain, $R_m$, approaches infinity, and applying external negative feedback will force the two input currents, $I_+$ and $I_-$ to be equal.

The OTRA can be realized using two CFOAs as shown in Fig. 7(b).

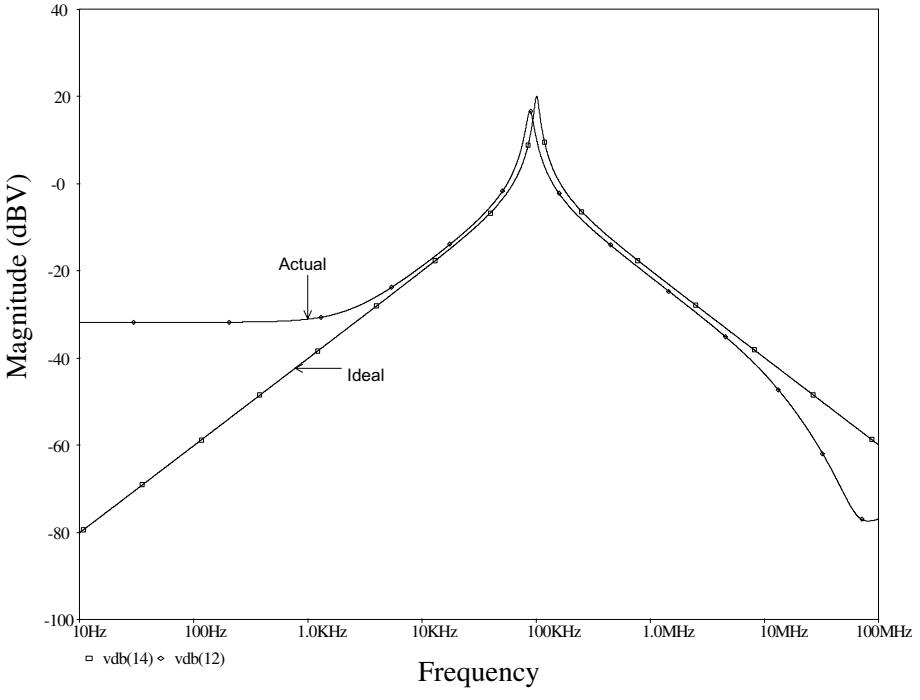


Fig. 6(b). Ideal and actual magnitude responses of KHN using AD844 and MOS-C with $Q = 10$, $f_0 = 100\,\text{KHz}$.

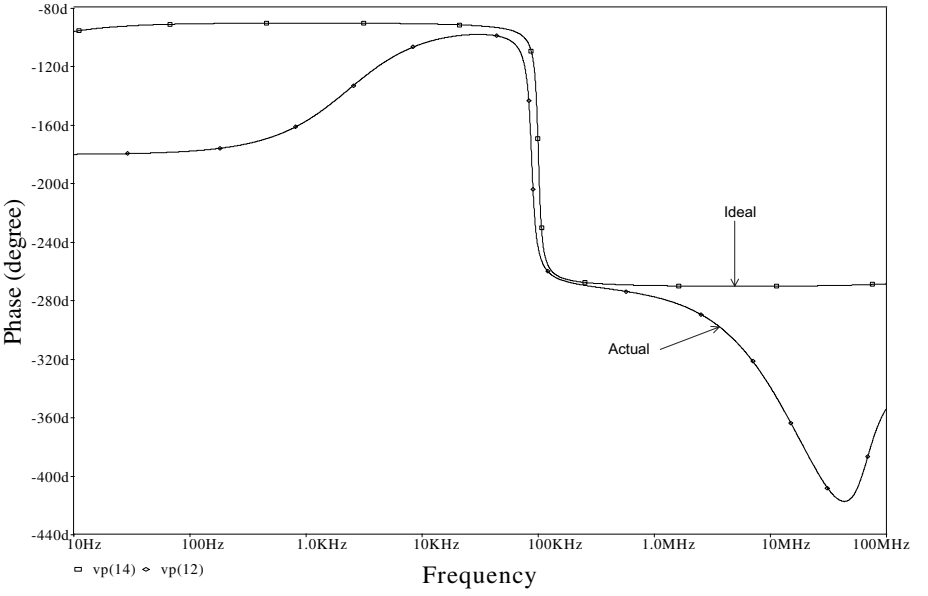


Fig. 6(c). Ideal and actual phase response of the band-pass KHN using AD844 and MOS-C with $f_0 = 100\,\text{KHz}$.

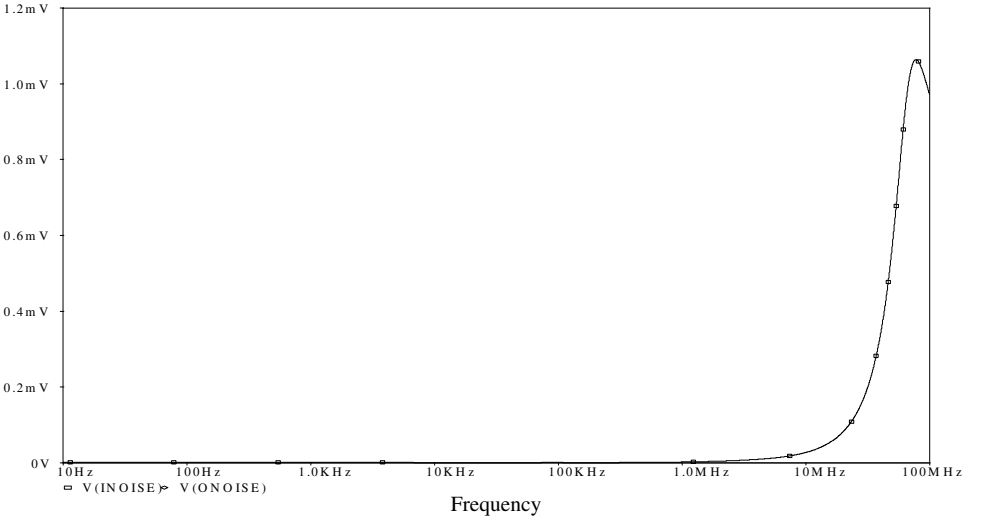


Fig. 6(d). The input/output referred noise of the KHN circuit of Fig. 6(a).

Figures 7(c) and 7(d) represent the active RC and the MOS-C KHN circuits using two OTRAs.

The PSpice simulations have been carried out for the circuit of Fig. 7(d) using the same design values as in the previous sections.

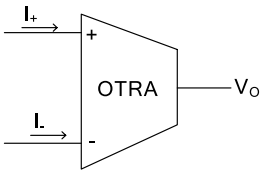


Fig. 7(a). OTRA symbol.

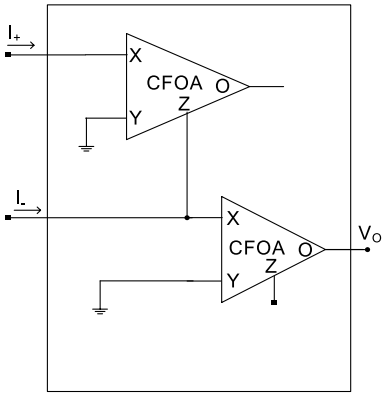


Fig. 7(b). OTRA implementation using CFOAs.[14]

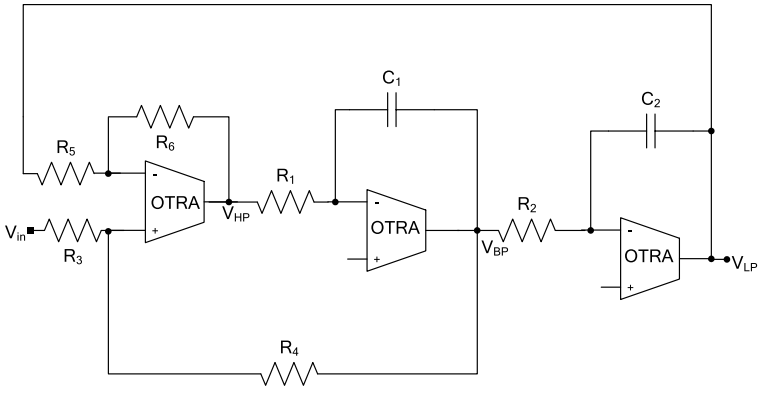


Fig. 7(c). KHN filter using OTRA and RC.

Figures 7(e) and 7(f) show the magnitude and phase responses of the simulated and the ideal responses respectively.

Figure 7(g) shows the input/output referred noise.

It is worth noting that eight alternative sign combinations of the high-pass, band-pass and low-pass polarities by proper choice of the signs of $V_{Gi}$ ($i = 1$ to 4) as explained in Ref. 15.

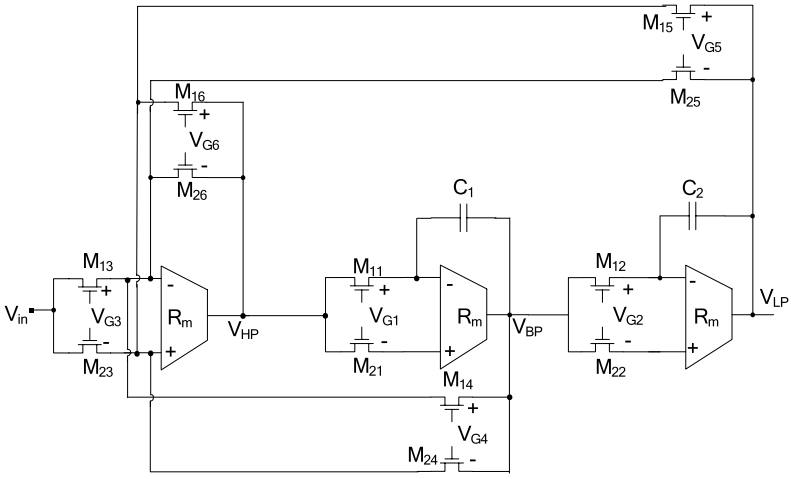


Fig. 7(d). KHN filter using OTRA and MOS-C.[15]

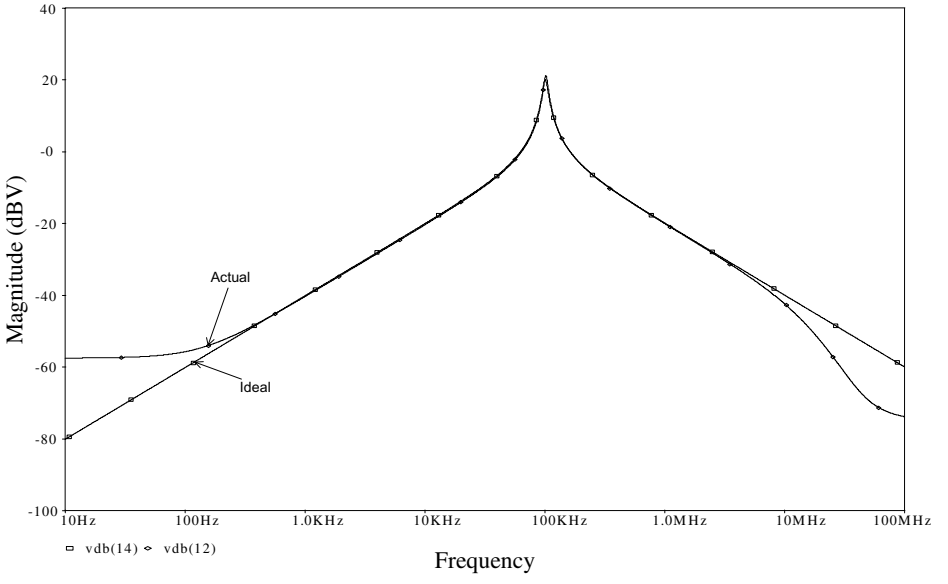


Fig. 7(e). Ideal and actual magnitude responses of KHN using OTRA and MOS-C with $Q = 10$, $f_0 = 100\,\text{KHz}$.

## 7. MOS-C KHN Circuit Using DCVC

The DCVC is a versatile four-terminal analog building block[15] based on cascaded connection of Modified Differential Current Conveyor MDCC[16] and a voltage follower. The DCVC is represented symbolically as shown in Fig. 8(a). It is

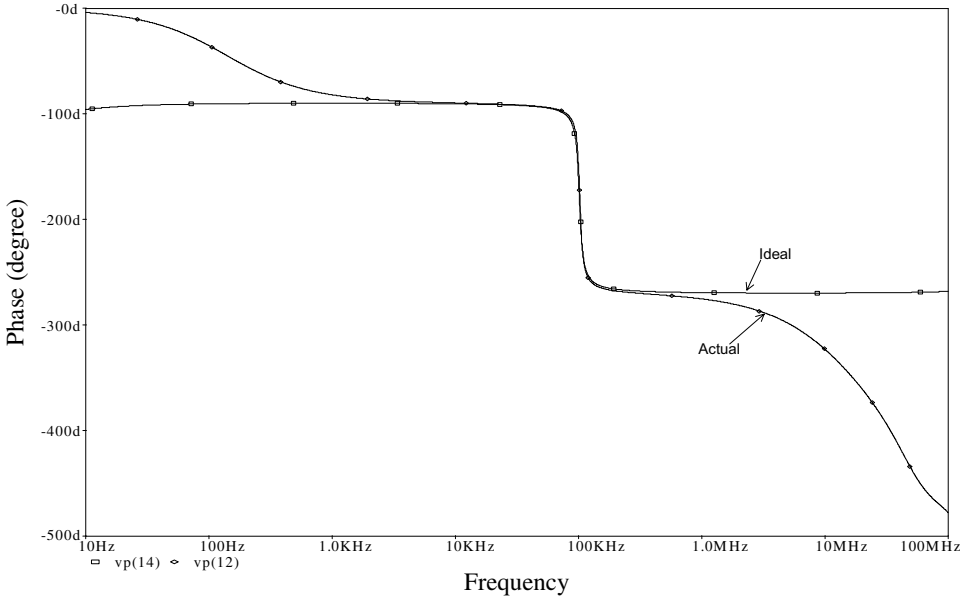


Fig. 7(f). Ideal and actual phase response of the band-pass KHN using OTRA and MOS-C with $f_0 = 100\,\text{KHz}$.

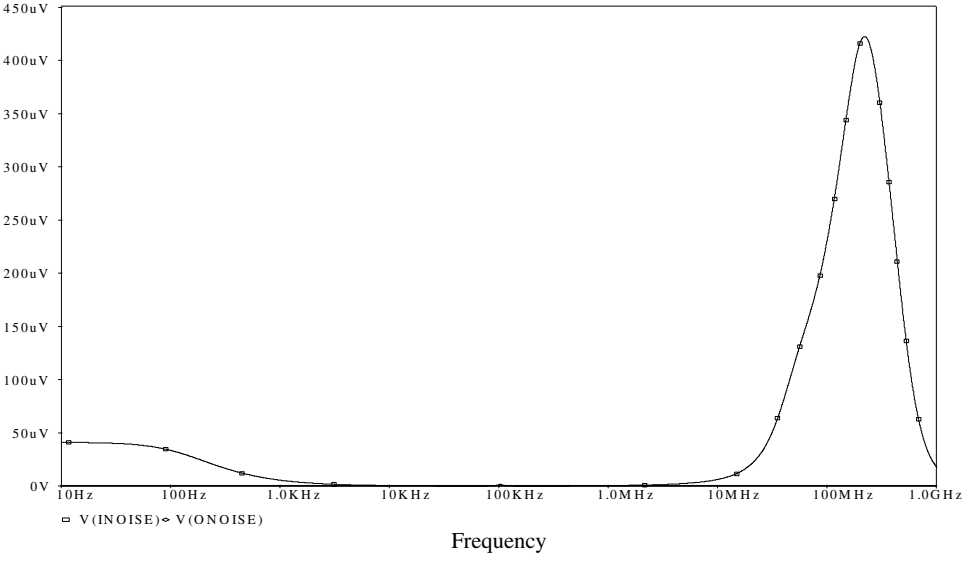


Fig. 7(g). The input/output referred noise of the KHN of Fig. 7(c).

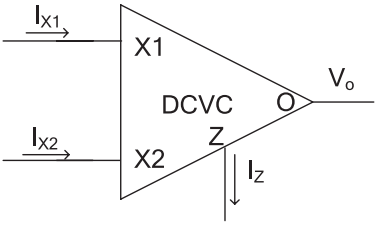


Fig. 8(a). DCVC symbol.

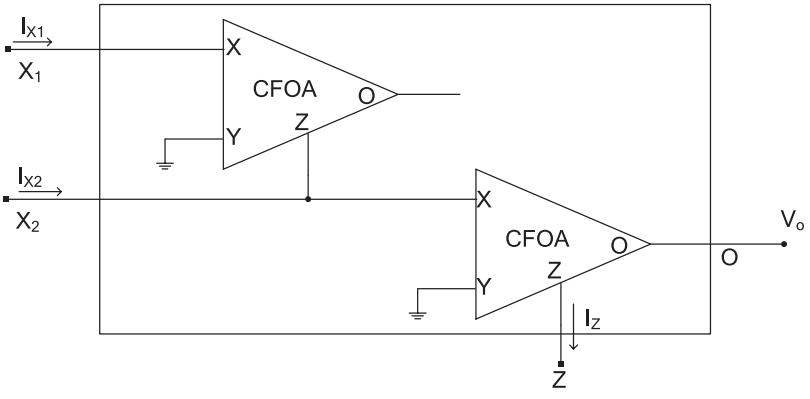


Fig. 8(b). DCVC implementation using CFOAs.

characterized by the following matrix equation:

$$\begin{bmatrix} V_{X1} \\ V_{X2} \\ I_Z \\ V_O \end{bmatrix} = \begin{bmatrix} 0 & 0 & 0 & 0 \\ 0 & 0 & 0 & 0 \\ 1 & -1 & 0 & 0 \\ 0 & 0 & 1 & 0 \end{bmatrix} \begin{bmatrix} I_{X1} \\ I_{X2} \\ V_Z \\ I_O \end{bmatrix}. \tag{24}$$

The circuit equations are the same as given by Eqs. (13)–(17).

The DCVC can be realized using two CFOAs as shown in Fig. 8(b).

The PSpice simulations have been carried out for the circuit of Fig. 8(c) using the same design values as in the previous sections.

Figures 8(d) and 8(e) show the magnitude and phase responses of the simulated and the ideal responses respectively from simulating the KHN using DCVC satisfing the requirements of the required filter. Figure 8(f) shows the input/output referred noise.

It is worth noting that eight alternative sign combinations of the high-pass, band-pass and low-pass polarities by proper choice of the signs of $V_{Gi}$ ($i = 1$ to 4) as explained in Ref. 16.

Tables 2 and 3 include comparison between different MOS-C KHN circuits using the commercially available VOA and CFOA.

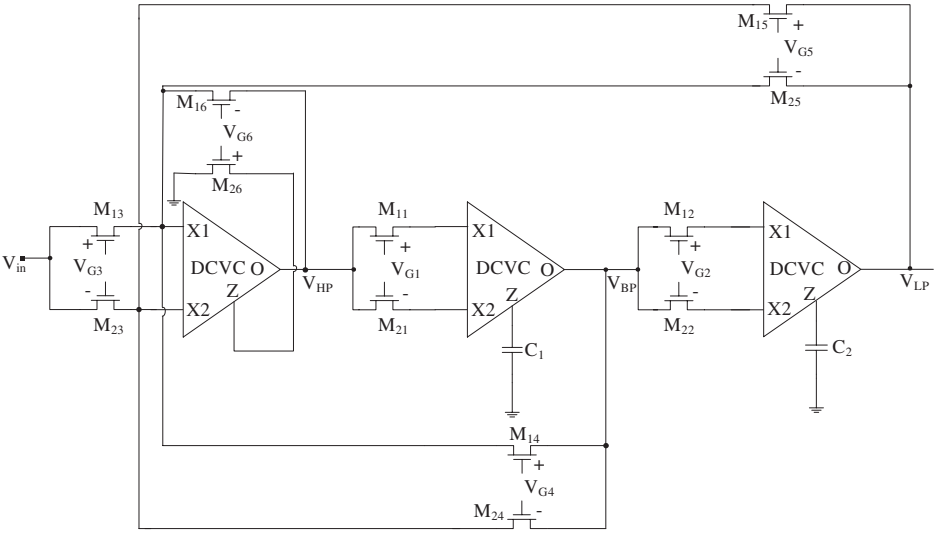


Fig. 8(c). KHN filter using DCVC and MOS-C.[18]

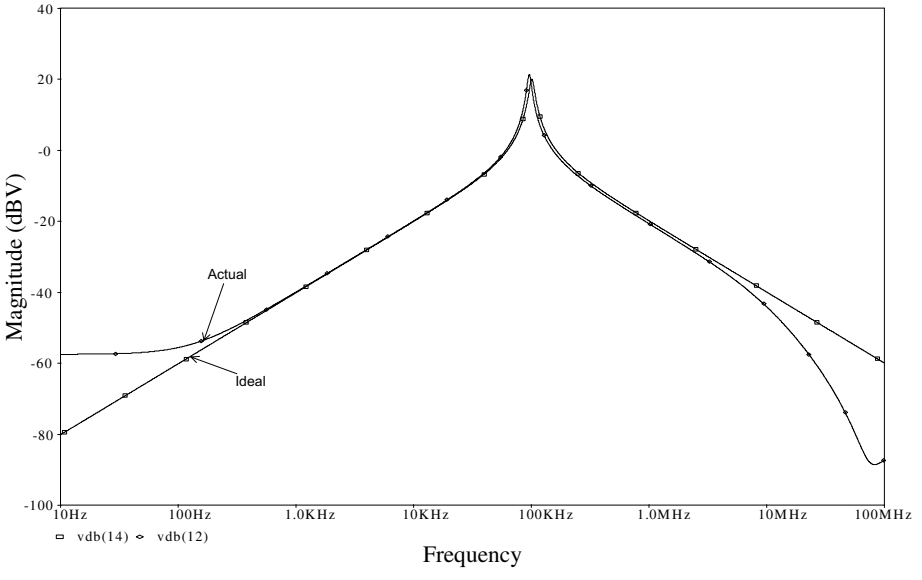


Fig. 8(d). Ideal and actual magnitude responses of KHN using DCVC and MOS-C with $Q = 10$, $f_0 = 1\,\text{MHz}$.

## 8. MOS-C KHN Circuit Using CMOS-VOA

In this section the CMOS-VOA given in Ref. 19 and shown here in Fig. 9(a) is used as the active building block in the KHN circuit. The compensating capacitor $C_c$ is taken as 2.5 pF and the compensating resistor $R_c$ is taken as 10 kΩ. Table 4

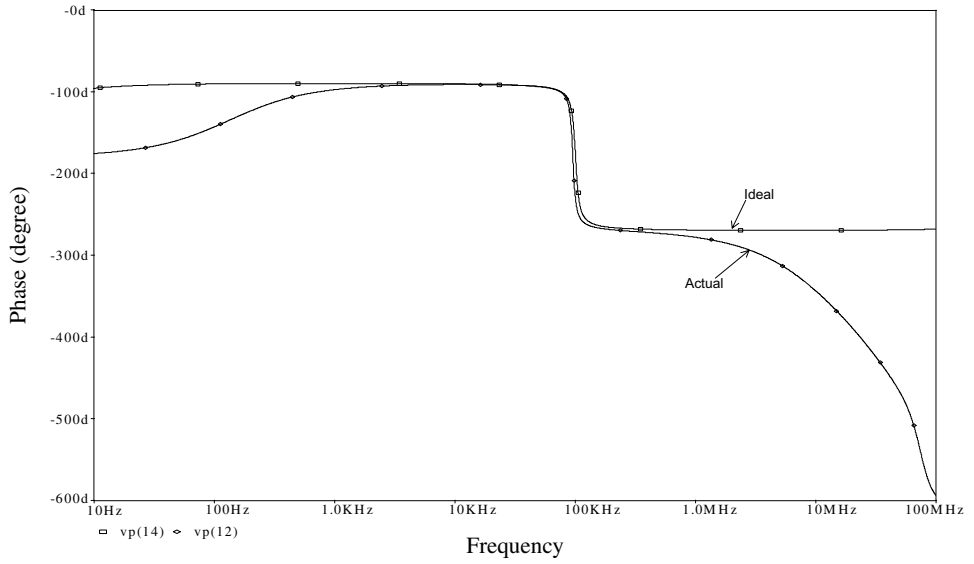


Fig. 8(e). Ideal and actual phase response of the band-pass KHN using DCVC and MOS-C with $f_0 = 1\,\text{MHz}$.

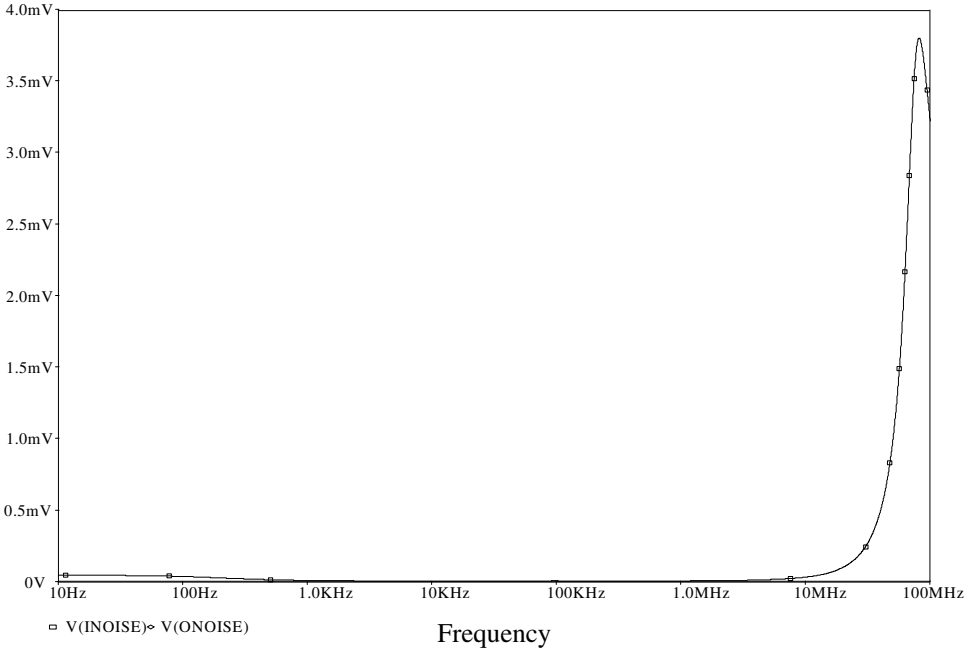


Fig. 8(f). The input/output referred noise of the KHN of Fig. 8(c).

Table 2. Summary of MOS-C KHN simulation results using VOA and CFOA.

| | Fig. 3(b)[10] | Fig. 5(a) | Fig. 6(a) | Fig. 7(d)[14] | Fig. 8(c)[15] |
|---|---|---|---|---|---|
| No. of capacitors | | | | | |
| Grounded | 2 | 2 | 2 | 0 | 2 |
| Floating | 2 | 2 | 0 | 2 | 0 |
| Number/Type of active elements | 3/LM741* | 3/AD844† | 3/AD844 | 6/AD844 | 6/AD844 |
| Number of transistors | 24 | 24 | 24 | 12 | 12 |
| Power supplies ($V_{dd}$, $V_{ss}$) | 12 V, −12 V | 5 V, −5 V | 5 V, −5 V | 5 V, −5 V | 5 V, −5 V |
| Power consumption | 117 mW | 211 mW | 211 mW | 421 mW | 421 mW |
| Input referred noise $\mu V/\sqrt{Hz}$ | 128.375 | 821.774 | 1063.6 | 422.725 | 3799.6 |
| Output referred noise $\mu V/\sqrt{Hz}$ | 0.147249 | 2.0453 | 2.0717 | 1.8641 | 4.065 |

*LM741 macro model provided by National Semiconductor.
†AD844 macro model provided by Analog Devices.

Table 3. Percentage errors from the ideal frequency and gain ($f_{0ideal} = 100$ KHz).

| | $f_{0Actual}$ (KHz) | %error in gain | %error in $f_0$ |
|---|---|---|---|
| Fig. 3(b)[10] | 86.696 | −60% | −14.49% |
| Fig. 5(a) | 100.231 | −3.96% | −1.14% |
| Fig. 6(a) | 88.512 | −16.9% | −12.7% |
| Fig. 7(d)[14] | 102.329 | +6.25% | 0.925% |
| Fig. 8(c)[15] | 96.161 | +6.96% | −5.16% |

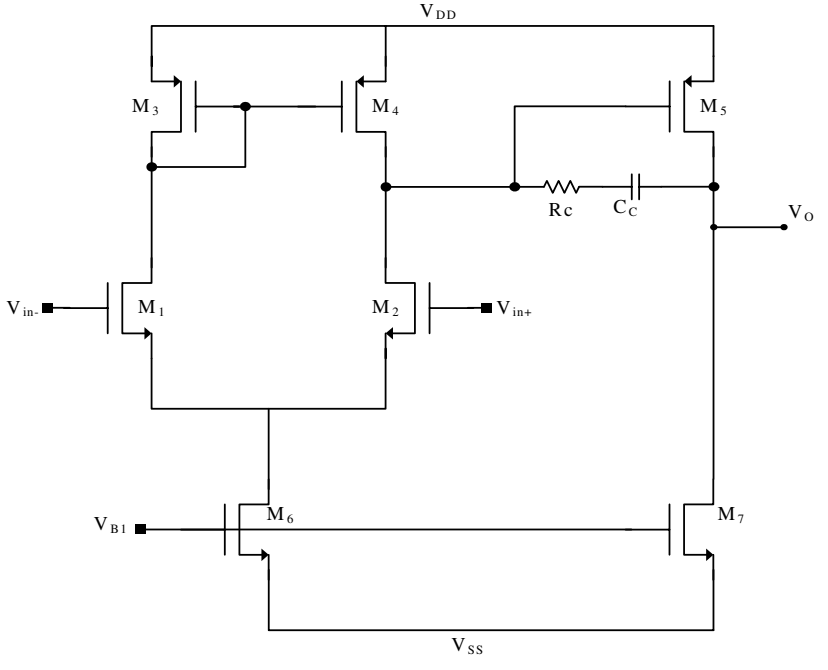


Fig. 9(a). CMOS realization of the op-amp[19] used to realize KHN circuit.

Table 4. Aspect ratio of the transistors of the CMOS-VOA circuit shown in Fig. 9(a).[19]

| Transistors | $W$ ($\mu$m) | $L$ ($\mu$m) |
|---|---|---|
| $M_1$, $M_2$ | 56 | 3.6 |
| $M_3$, $M_4$, $M_5$ | 90 | 4.8 |
| $M_7$, $M_8$ | 0.18 | 1.8 |

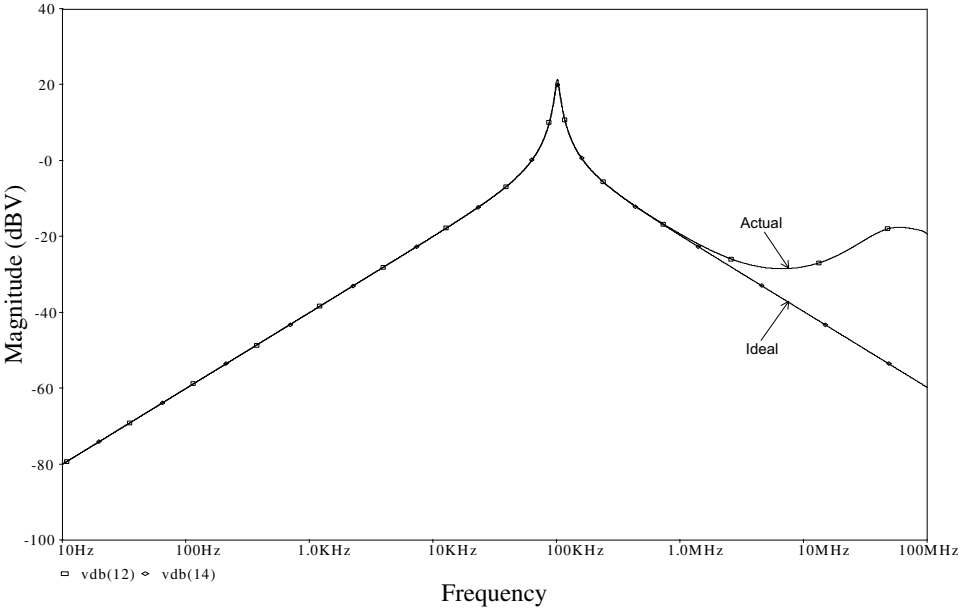


Fig. 9(b). Magnitude responses of KHN using CMOS-VOA and MOS-C.

includes the transistor aspect ratios of the CMOS circuit of Fig. 9(a). This CMOS-VOA circuit is used in the KHN circuit shown in Fig. 3(b).

The PSpice simulations have been carried out using 0.18 CMOS technology model from MOSIS to realize a band-pass response with $f_0 = 100\,\text{kHz}$ and $Q = 10$. The design values of the circuit parameters are taken as in the previous sections. The CMOS-VOA is used with supply voltages of $\pm 1.5\,\text{V}$ and $V_{B1}$ of $-1\,\text{V}$.

Figures 9(b) and 9(c) show the magnitude and phase responses of the simulated and the ideal responses respectively. It is seen that both responses are much better than those shown in Fig. 3 with the commercially available VOA. Figure 9(d) shows the input/output referred noise.

Figures 9(e) and 9(f) show the magnitude and phase responses of the simulated and the ideal low-pass responses designed for $f_0 = 1\,\text{MHz}$ and $Q = 0.707$ and $DC$ gain = 2.

The design values of the circuit parameters are $C_1 = C_2 = 54.5\,\text{pF}$. The transistor aspect ratios $(W/L) = (2\,\mu\text{m}/4\,\mu\text{m})$, $K^{\backslash} = 251.497\,\mu\text{A/V}^2$, and the gate

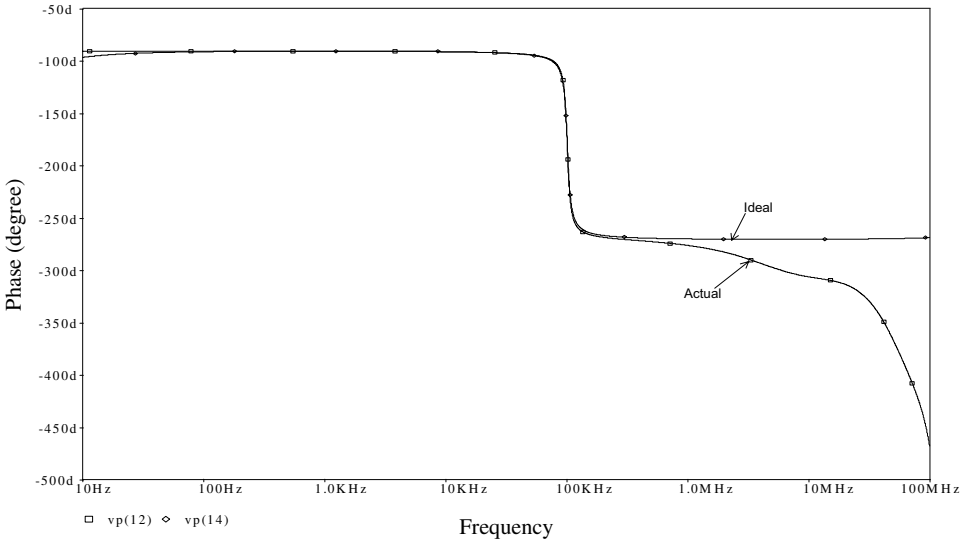


Fig. 9(c). Phase responses of KHN using CMOS-VOA and MOS-C.

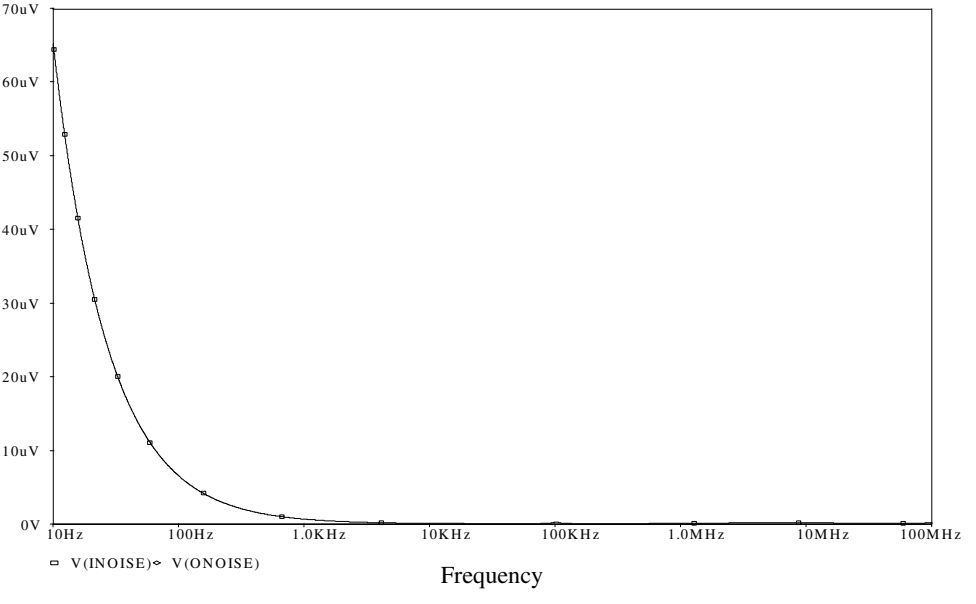


Fig. 9(d). The input/output referred noise of the KHN using CMOS-VOA and MOS-C.

voltages have been taken as $V_{G1} = V_{G2} = V_{G5} = V_{G6} = 2.748\,\text{V}$, $V_{G3} = 5.496$ and $V_{G4} = 3.89\,\text{V}$. The CMOS-VOA is used with supply voltages of $\pm 1.5\,\text{V}$ and $V_{B1}$ of $-1\,\text{V}$. The magnitude and phase simulated results are very close to the ideal ones.

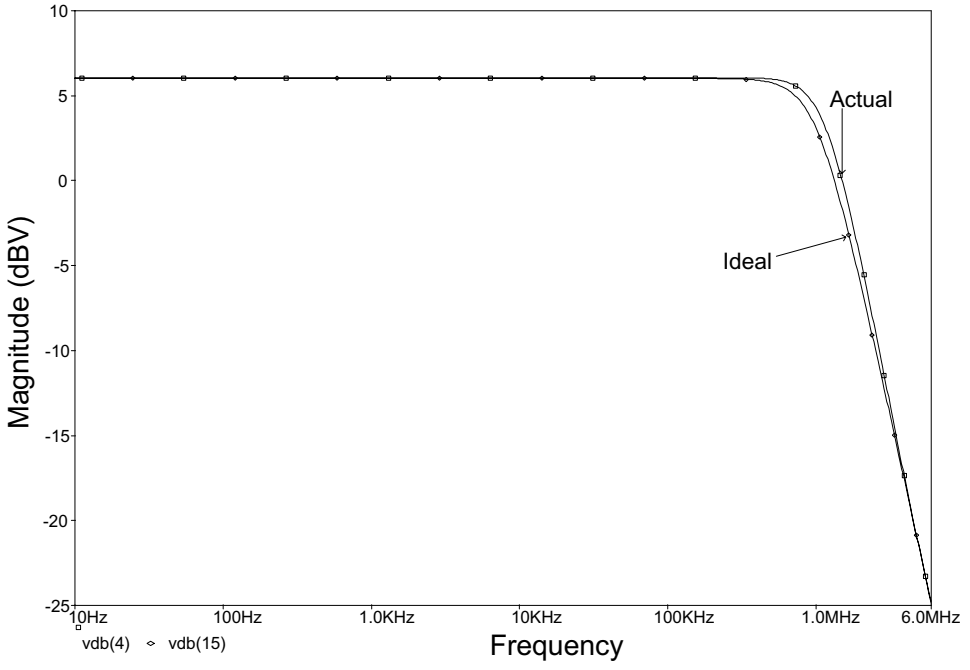


Fig. 9(e). Magnitude responses of low-pass KHN output using CMOS-VOA and MOS-C.

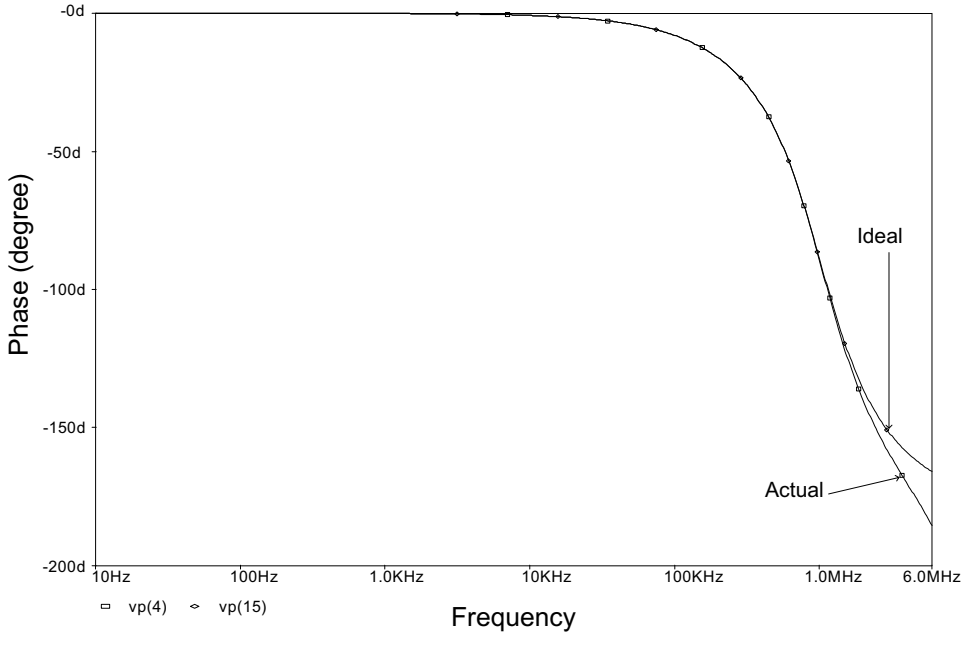


Fig. 9(f). Phase responses of low-pass KHN output using CMOS-VOA and MOS-C.

## 9. MOS-C KHN Circuit Using CMOS-CFOA

In this section the CMOS-CFOA given in Ref. 20 and shown here in Fig. 10(a) is used as the active building block in the KHN circuit of Fig. 6(a). Table 5 includes the transistor aspect ratios of the CMOS circuit of Fig. 10(a).

The PSpice simulations have been carried out using 0.18 CMOS technology model from MOSIS to realize a band-pass response with $f_0 = 100\,\text{kHz}$ and $Q = 10$. The design values of the circuit parameters are the same as in the previous circuit. The CMOS-CFOA is used with supply voltages of $\pm 1.5\,\text{V}$. $V_C$ and $V_{B1}$ are taken $1.4\,\text{V}$ and $-0.8\,\text{V}$ respectively.

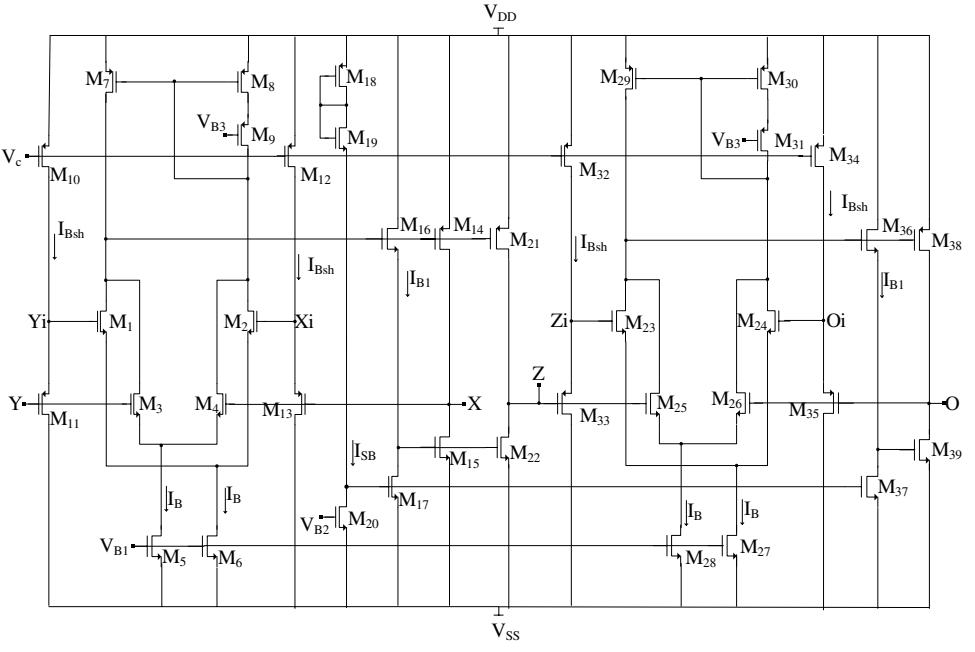


Fig. 10(a). CMOS realization of the CFOA[20] used to realize KHN circuit.

Table 5. Aspect ratio of the transistors of the CFOA shown in Fig. 10(a).[20]

| Transistors | $W$ ($\mu$m) | $L$ ($\mu$m) |
|---|---|---|
| $M_1$–$M_4$, $M_{23}$–$M_{26}$ | 1.8 | 0.72 |
| $M_5$, $M_6$, $M_{27}$, $M_{28}$ | 5.2 | 0.72 |
| $M_7$, $M_8$, $M_{29}$, $M_{30}$ | 110 | 3.6 |
| $M_{10}$–$M_{13}$, $M_{32}$–$M_{35}$ | 140 | 3.6 |
| $M_{18}$–$M_{20}$ | 3.6 | 3.6 |
| $M_{16}$, $M_{17}$, $M_{36}$, $M_{37}$ | 1 | 1 |
| $M_{14}$, $M_{21}$, $M_{38}$ | 37 | 3.6 |
| $M_{15}$, $M_{22}$, $M_{39}$ | 30 | 3.6 |

Figures 10(b) and 10(c) show the magnitude and phase responses of the simulated and the ideal responses respectively. It is seen that both responses are much better than those shown in Fig. 3 with the commercially available CFOA. Figure 10(d) shows the input/output referred noise.

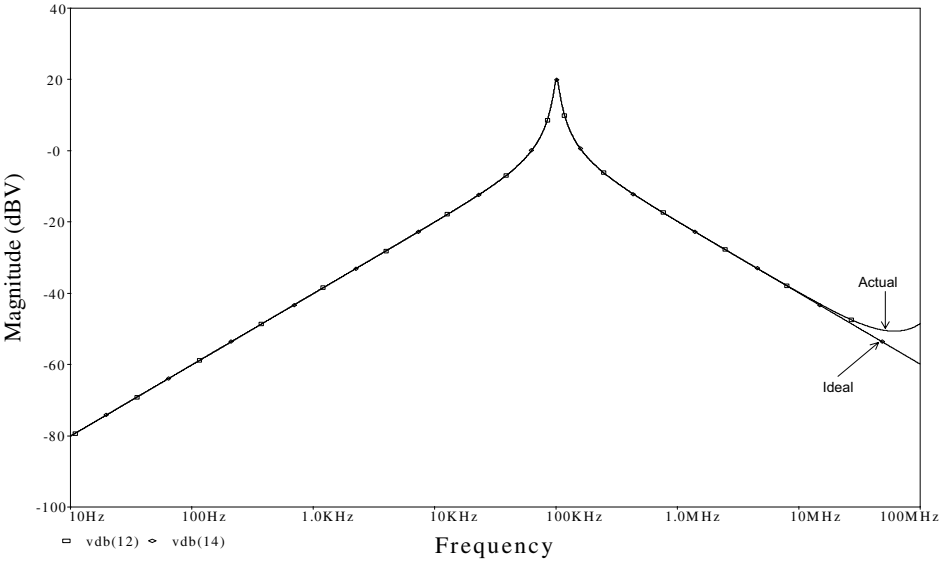


Fig. 10(b). Magnitude responses of KHN using CMOS-CFOA and MOS-C.

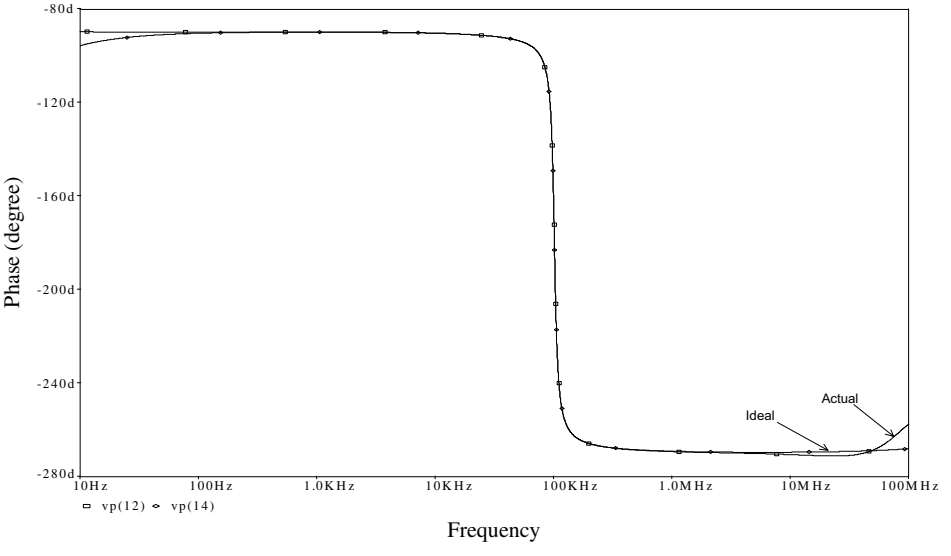


Fig. 10(c). Phase responses of KHN using CMOS-CFOA and MOS-C.

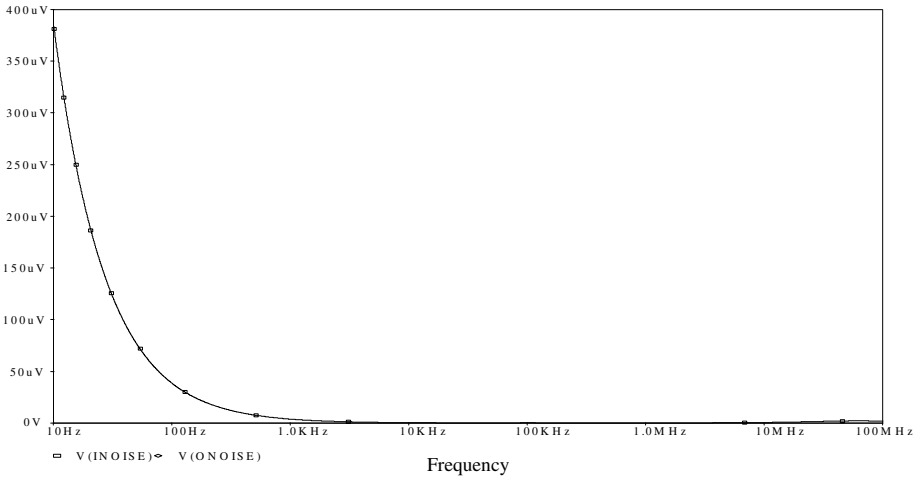


Fig. 10(d). The input/output referred noise of the KHN using CMOS-CFOA and MOS-C.

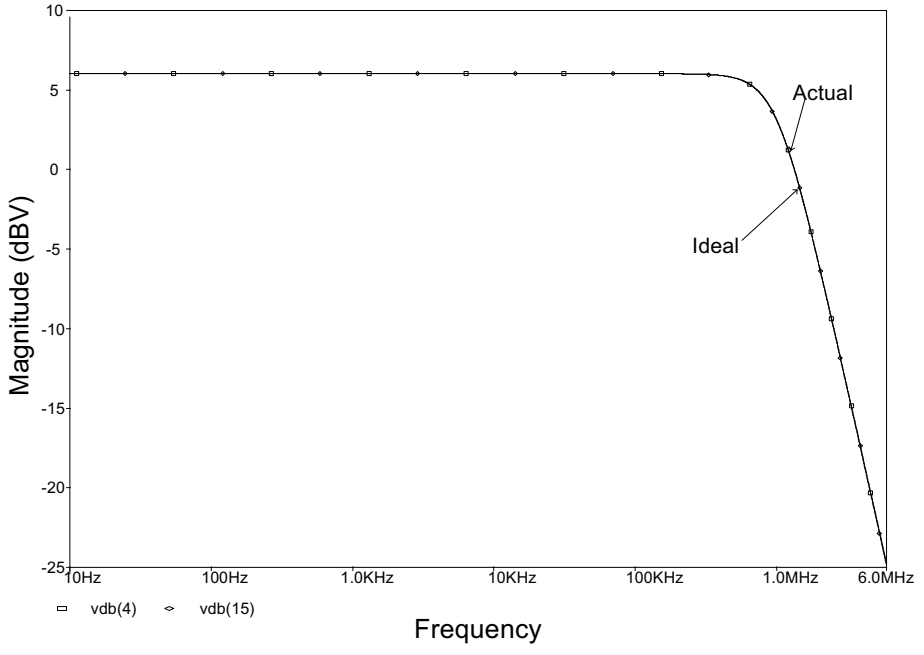


Fig. 10(e). Magnitude responses of low-pass KHN output using CMOS-CFOA and MOS-C.

Figures 10(e) and 10(f) show the magnitude and phase responses of the simulated and the ideal low-pass responses designed for $f_0 = 1\,\text{MHz}$ and $Q = 0.707$ and *DC* gain = 2. The design values are taken as in the case of the CMOS-VOA. The magnitude and phase simulated results are very close to the ideal ones.

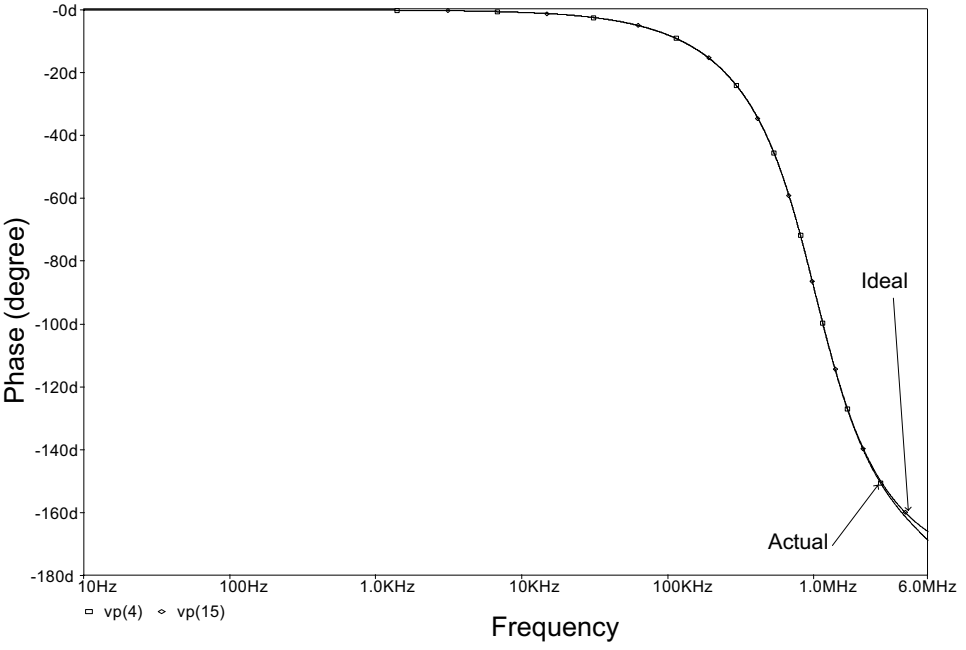


Fig. 10(f). Phase responses of low-pass KHN output using CMOS-CFOA and MOS-C.

## 10. MOS-C KHN Circuit Using CMOS-OTRA

In this section the CMOS-OTRA given in Ref. 21 and shown here in Fig. 11(a) is used as the active building block in the KHN circuit shown in Fig. 7(d). Table 6 includes the transistor aspect ratios of the CMOS circuit of Fig. 11(a).

The PSpice simulations have been carried out using 0.18 CMOS technology model from MOSIS to realize a band-pass response with $f_0 = 100\,\text{kHz}$ and $Q = 10$. The design values of the circuit parameters are the same as in the previous circuit. The CMOS-OTRA is used with supply voltages of $\pm 1.5\,\text{V}$ and $V_{B1}$ of $-0.9\,\text{V}$. Figures 11(b) and 11(c) show the magnitude and phase responses of the simulated and the ideal responses respectively. Figure 11(d) shows the input/output referred noise.

## 11. Comparison with Gm-C KHN Filter

Two very popular methods of realizing linear filters are the transconductance-C (Gm-C) method and the switched capacitor (SC) method. SC filters are discrete time filters which use capacitors and MOS switches to realize transfer functions in a discrete time domain. SC filters are highly linear but have a limited frequency response. In particular the presence of Op Amps with their limited bandwidth and large parasitics cause SC filters to become impractical at high frequencies.

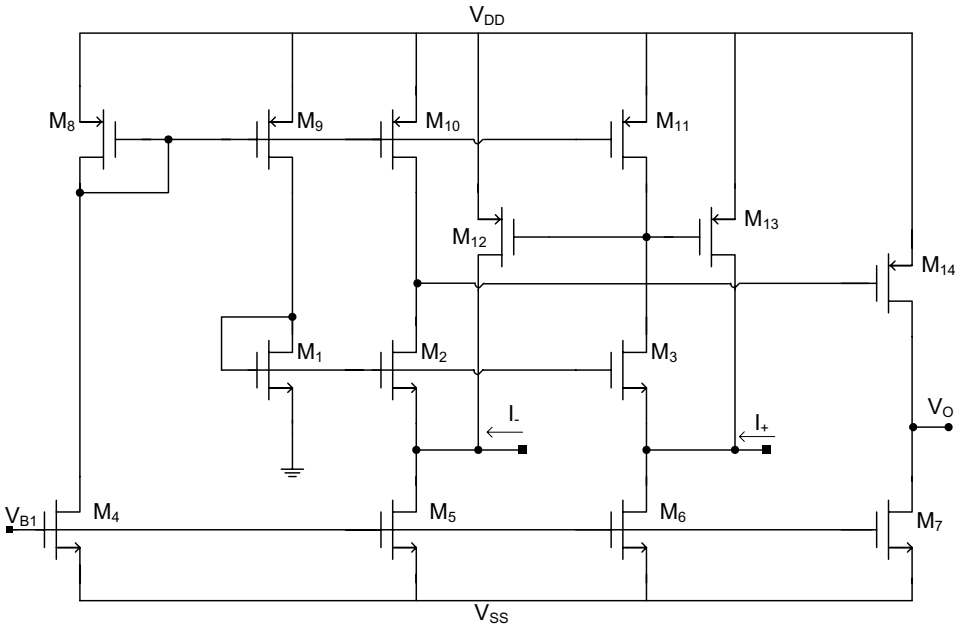


Fig. 11(a). CMOS realization of the OTRA[21] used to realize KHN circuit.

Table 6. Aspect ratio of the transistors of the OTRA circuit shown in Fig. 11(a).[21]

| Transistors | $W$ ($\mu$m) | $L$ ($\mu$m) |
|---|---|---|
| $M_1$–$M_3$, $M_{12}$, $M_{13}$ | 100 | 1.8 |
| $M_4$, $M_7$ | 10 | 1.8 |
| $M_5$, $M_6$ | 30 | 1.8 |
| $M_8$–$M_{11}$ | 50 | 1.8 |
| $M_{14}$ | 50 | 3.6 |

The Gm-C filters use simple building blocks with few internal nodes and thus limited parasitics. The main building block in these filters is a linear transconductor. Transconductors are essentially uncomplicated and include fewer internal nodes than Op Amps. Gm-C filters can give good responses at high frequencies this comes at the expense of linearity. Transconductors are never perfectly linear their characteristics show clear nonlinear components that cannot be ignored. Therefore if a filter is to function properly each transconductor must be liberalized[22,23] on its own thus increasing the filter complexity.

For comparison purposes the Gm-CKHN filter is given in Fig. 12(a),[24] the circuit uses eight transconductors and two grounded capacitors. The Gm and the capacitors are numbered properly so that Eqs. (9)–(11) apply to this circuit

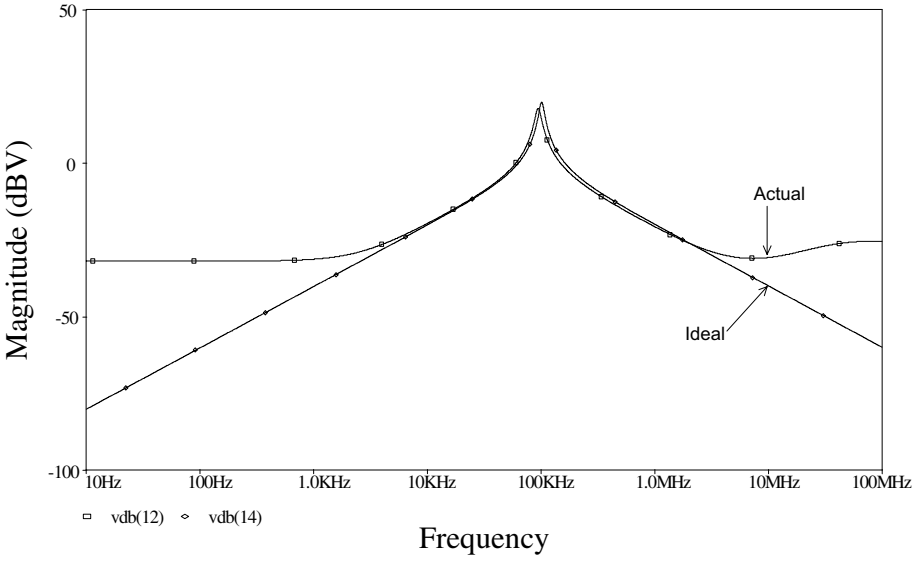


Fig. 11(b). Ideal and actual magnitude responses of KHN using CMOS-OTRA and MOS-C.

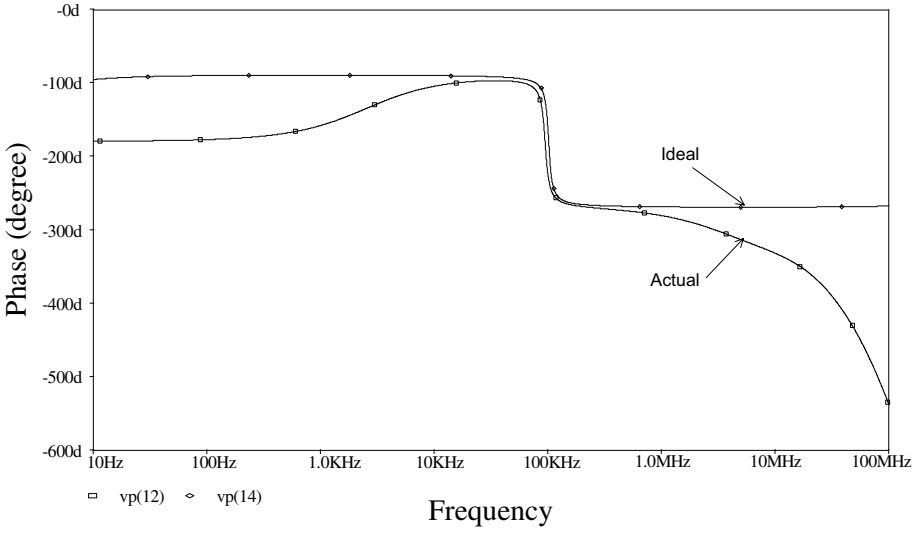


Fig. 11(c). Ideal and actual phase responses of KHN using CMOS-OTRA and MOS-C.

provided that $G_7$ and $G_8$ are taken equal. For a simplified design, the design equations are given by:

$$C_1 = C_2 = C\,, \quad G_1 = G_2 = G_5 = G_6 = G\,, \tag{25a}$$

$$G = \omega_0 C\,, \quad G_4 = \frac{G}{Q}\,. \tag{25b}$$

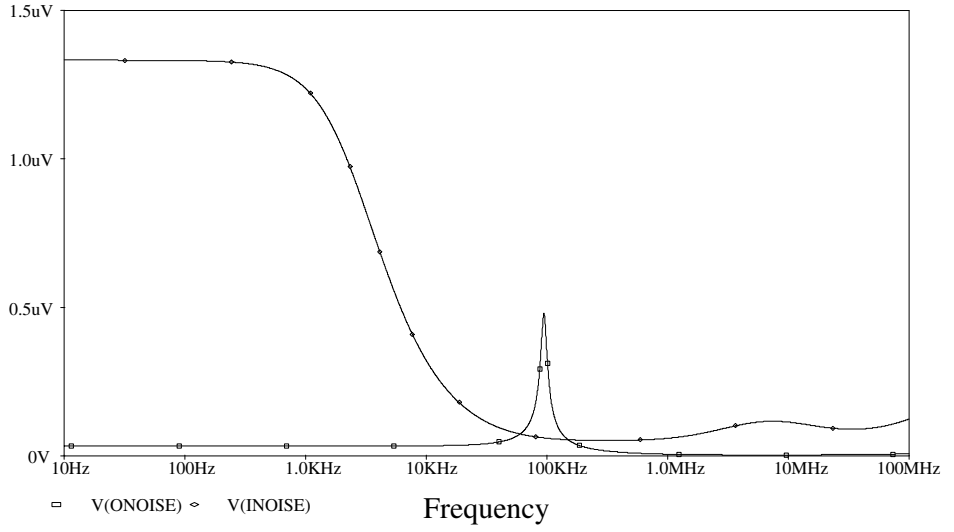


Fig. 11(d). The input/output referred noise of the KHN using CMOS-OTRA and MOS-C.

For a specified *DC* gain:

$$G_3 = (\text{DC gain})G_5\,. \tag{26a}$$

For a band-pass filter with a specified center frequency gain:

$$G_3 = \text{Gain}(\omega_0)G_4\,. \tag{26b}$$

The PSpice simulations have been carried out using 0.18 CMOS technology model from MOSIS and the CMOS-transconductor used is shown in Fig. 12(b) and with supply voltages of $\pm\,1.5\,\text{V}$ and the transistor aspect ratios is given in Table 7.

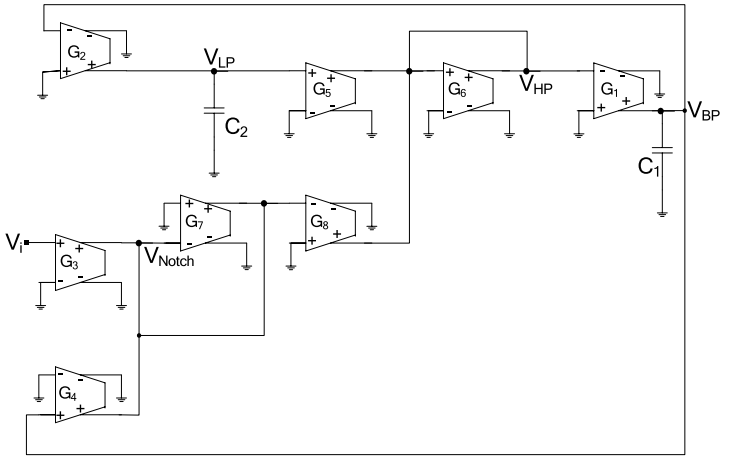


Fig. 12(a). Voltage-mode Gm-C version of the KHN filter.[24]

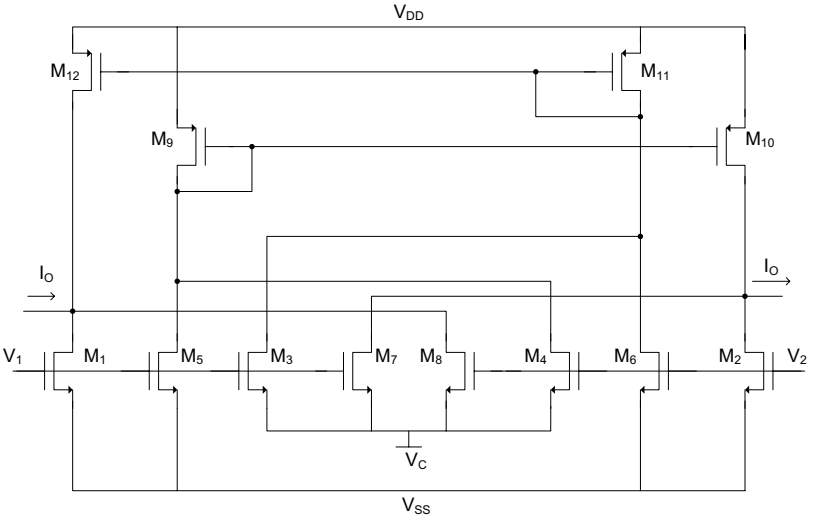


Fig. 12(b). CMOS realization of the transconductor used in Fig. 12(a).[25]

Table 7. Aspect ratio of transconductor in Fig. 12(b).

| Transistor | $W$ ($\mu$m) | $L$ ($\mu$m) |
|---|---|---|
| $M_1$–$M_8$ | 1.8 | 3.6 |
| $M_9$–$M_{12}$ | 14 | 3.6 |

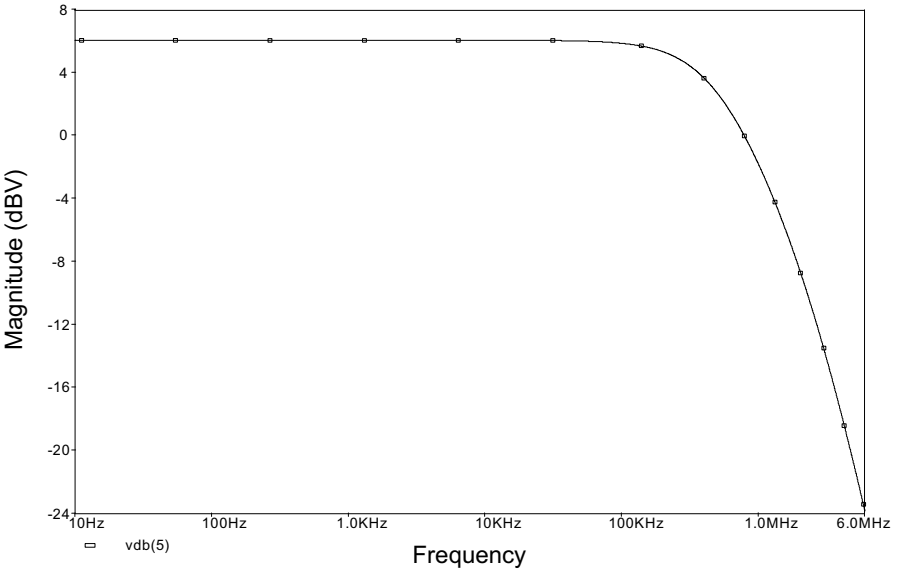


Fig. 12(c). Magnitude response of the Gm-C filter at $f_0 = 1\,\text{MHz}$, gain $= 2$ and $Q = 0.707$.

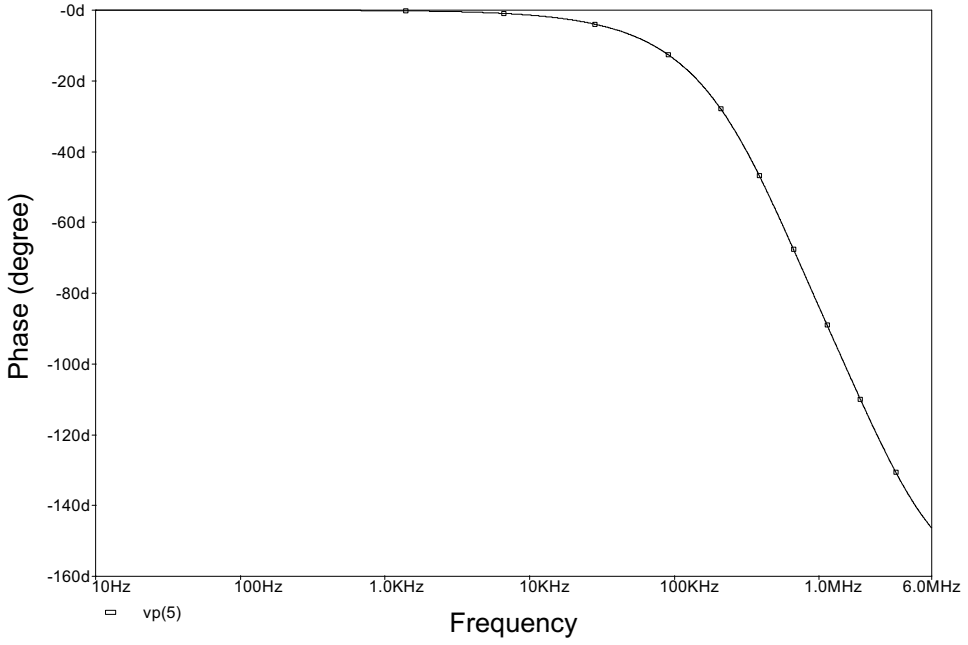


Fig. 12(d). Phase response of the Gm-C filter.

Table 8. Summary of KHN MOS-C simulation results using CMOS-VOA, CMOS-CFOA and CMOS-OTRA active blocks.

| Active building block | CMOS-VOA Fig. 9(a)[19] | CMOS-CFOA Fig. 10(a)[20] | CMOS-OTRA Fig. 11(a)[21] |
|---|---|---|---|
| Power supplies ($V_{DD}$, $V_{SS}$) | 1.5 V, −1.5 V | 1.5 V, −1.5 V | 1.5 V, −1.5 V |
| Power consumption | 2.84 mW | 91.9 mW | 18.1 mW |
| Input referred noise $\mu V/\sqrt{Hz}$ | 65 | 400 | 1.33 |
| Output referred noise $\mu V/\sqrt{Hz}$ | 0.276 | 0.692 | 0.481 |
| THD@100 KHz | 15.6% | 12.5% | 17.1% |

Table 9. Summary of MOS-C KHN simulation results using CMOS-VOA, CMOS-CFOA and CMOS-TA active blocks for low-pass output.

| Active building block | CMOS-VOA Fig. 9(a)[19] | CMOS-CFOA Fig. 10(a)[20] | CMOS-OTRA Fig. 12(a)[22] |
|---|---|---|---|
| Power supplies ($V_{DD}$, $V_{SS}$) | 1.5 V, −1.5 V | 1.5 V, −1.5 V | 1.5 V, −1.5 V |
| Power consumption | 2.84 mW | 91.9 mW | 35.1 mW |
| Input referred noise $\mu V/\sqrt{Hz}$ | 0.255 | 0.166 | 0.173 |
| Output referred noise $\mu V/\sqrt{Hz}$ | 0.03697 | 0.0837 | 0.0018 |
| THD@1 MHz | 37.3% | 9.79% | 22.68% |

Figures 12(c) and 12(d) show the magnitude and phase responses of the simulated low-pass response designed for $f_0 = 1\,\text{MHz}$ and $Q = 0.707$ and $DC$ gain $= 2$. The design values taken are $C_1 = C_2 = 17.145\,\text{pF}$, $G_1 = G_2 = G_5 = G_6 = G_7 = G_8 = 62.874\,\mu\text{A/V}$ and $G_3 = 125.7485\,\mu\text{A/V}$, $G_4 = 88.931\,\mu\text{A/V}$. The magnitude of the transconductors is adjusted by the control voltage $V_C$ and for $G_1$, $G_2$, $G_5$, $G_7$, $G_8$ the voltage $V_C$ is taken $-1\,\text{V}$. For $G_4$ the voltage $V_C$ is taken $-0.086\,\text{V}$ and for $G_3$ the voltage $V_C$ is taken $-0.5\,\text{V}$.

## 12. Conclusions

A detailed study of the MOS-C KHN circuits using the VOA, CFOA, OTRA and DCVC has been presented. Both the VOA and the CFOA with the $Z$ terminal open require four capacitors; two of them are floating and the VOA has the highest frequency and $Q$ deviations due to the finite gain bandwidth. A new canonic CFOA KHN circuit using grounded capacitors is introduced in this paper and is shown in Fig. 6(a).

The canonic KHN circuit using OTRA and shown in Fig. 7(d) uses only two capacitors but both of them are floating.[15] The DCVC MOS-C KHN circuit shown in Fig. 8(c) uses two grounded capacitors only. Of course this circuit is intended to be used with the CMOS-DCVC as the basic building block.[18]

Simulation results demonstrating the differences between circuits performance has been included.

Table 8 includes comparison between different MOS-C KHN circuits using CMOS-VOA, CMOS-CFOA and CMOS-OTRA.

It is seen the power consumption with CMOS active building blocks is much lower than the power consumption with the commercially available building blocks.

Table 9 includes summary of MOS-C KHN simulation results using CMOS-VOA, CMOS-CFOA and CMOS-TA active blocks for low-pass output. From Table 9; it is seen that the Gm-CKHN filter has lower THD than the VOA-KHN. The CMOS CFOA-KHN filter however has lower THD than the Gm-CKHN filter.

## References

1. W. Kerwin, L. Huelsman and R. W. Newcomb, State variable synthesis for insensitive integrated circuit transfer functions, *IEEE J. Solid-State Circuit* **2** (1967) 87–92.
2. A. Budak, *Passive and Active Network Analysis and Synthesis* (Houghton Mifflin, 1974), pp. 356–365.
3. M. S. Ghausi and K. R. Laker, *Modern Filter Design, Active RC and Switched Capacitor* (Prentice-Hall, New Jersey, 1981), pp. 226–227.
4. M. E. Van Valkenburg, *Analog Filter Design* (Holt Rinehart and Winston, 1982), pp. 136–137.
5. T. Deliyannis, Y. Sun and J. K. Fidler, *Continuous Time Active Filter Design* (CRC Press, 1999), pp. 146–147.
6. A. M. Soliman, History and progress of the Kerwin–Huelsman–Newcomb filter: Generation and Op Amp realizations, *J. Circuits Syst. Comput.* **17** (2008) 637–658.

7. Z. Czarnul, Modification of Banu-Tsividis, Continuous-time integrator structure, *IEEE Trans. Circuits Syst.* **33** (1968) 714–716.
8. Z. Czarnul, Novel MOS resistive circuit for synthesis of fully integrated continuous-time filters, *IEEE Trans. Circuits Syst.* **33** (1986) 718–721.
9. Analog Devices, *Linear Products Data Book* (Norwood, 1990).
10. M. Ismail, S. Smith and R. Beale, a new MOSFET-C universal filter structure for VLSI, *IEEE J. Solid-State Circuits* **23** (1988) 183–194.
11. P. R. Geffe, RC amplifier resonators for active filters, *IEEE Trans. Circuit Theory* **15** (1968) 415–419.
12. A. M. Soliman, Applications of the current feedback operational amplifiers, *Analog Integr. Circuits Signal Process.* **11** (1996) 265–302.
13. S. Evans, *Current Feedback Op-Amp Applications Circuits Guide* (Comlinear Corporation, Fort Collins, 1998).
14. Y.-K. Lo and H.-C. Chien, Switch-controllable OTRA-based square/triangular waveform generator, *IEEE Trans. Circuits Syst.-II* **44** (2007) 1110–1114.
15. K. N. Salama and A. M. Soliman, Operational transresistance amplifier for analog signal processing, *Microelectron. J.* **30** (1999) 235–245.
16. K. N. Salama and A. M. Soliman, Voltage mode Kerwin–Huelsman–Newcomb circuit using CDBAs, *Frequenz* **54** (2000) 90–93.
17. H. O. Elwan and A. M. Soliman, A CMOS differential current conveyor and applications for analog VLSI, *Analog Integr. Circuits Signal Process.* **11** (1996) 35–45.
18. K. N. Salama, H. O. Elwan and A. M. Soliman, Parasitic-capacitance-insensitive voltage-mode MOSFET-C filters using differential current voltage conveyor, *Circuits Syst. Signal Process.* **20** (2001) 11–26.
19. G. Palmisano and G. Palumbo, An optimized compensation strategy for two-stage CMOS op amps, *IEEE Trans. Circuits Syst. CAS-I* **42** (1995) 178–182.
20. S. A. Mahmoud, A. H. Madian and A. M. Soliman, New low voltage CMOS current feedback operational amplifier and its application, *ETRI J.* **29** (2007) 212–218.
21. H. M. Hassan and A. M. Soliman, A modified CMOS realization of the operational transresistance amplifier (OTRA), *Frequenz* **60** (2006) 70–76.
22. A. M. Ismail and A. M. Soliman, Novel CMOS wide-linear range transconductance amplifier, *IEEE Trans. Circuits Syst. (CASI)* **47** (2000) 1248–1253.
23. A. M. Ismail and A. M. Soliman, Novel CMOS linear transconductance element using adaptively biased source-coupled differential pair, *Int. J. Electron. Commun.* (*AEU*) **54** (2000) 87–92.
24. P. V. Ananda Mohan, Generation of OTA-C filter structures from active RC filter structures, *IEEE Trans. Circuits Syst. CAS-I* **37** (1990) 656–660.
25. S. A. Mahmoud and A. M. Soliman, CMOS balanced output transconductor and applications for analog VLSI, *Microelectron. J.* **30** (1999) 29–39.